Food Hydrocolloids for Health 4 (2023) 100151

Contents lists available at ScienceDirect

Food Hydrocolloids for Health

journal homepage: www.elsevier.com/locate/fhfh

Characterization and encapsulation efficiency of zein nanoparticles loaded with chestnut fruit shell, cedar and sweetgum bark extracts

Dilara Konuk Takma [a], Semra Bozkurt [a], Mehmet Koç [a], Figen Korel [b], Hilal Şahin Nadeem [a,*]

[a] Department of Food Engineering, Faculty of Engineering, Aydın Adnan Menderes University, 09010, Aydın, Turkey
[b] Department of Food Engineering, Faculty of Engineering, İzmir Institute of Technology, 35430, İzmir, Turkey

ARTICLE INFO

Keywords:
Zein nanoparticles
Encapsulation
Shell/bark wastes
Nanoprecipitation
High-speed homogenization
Ultrasonic homogenization

ABSTRACT

Zein nanoparticles (ZNPs) loaded with bioactive extracts of chestnut (*Castanea sativa* Mill.) shell, cedar (*Cedrus libani*) and sweetgum (*Liquidambar orientalis*) bark wastes were produced using different methods. Nanoprecipitation, high-speed homogenization and ultrasonic homogenization allowed the fabrication of ZNPs with particle sizes smaller than 202.40 nm, 430.25 nm and 325.50 nm, respectively. The smallest nanoparticle size was achieved at 132.81 nm for sweetgum bark extract-loaded ZNPs obtained by the nanoprecipitation method. Encapsulation efficiency (EE) was between 34.03 and 96.83% for all zein nanoparticles fabricated under different mixtures and process conditions. Zein concentration and extract ratio played an essential role in the EE of nanoparticles. The best conditions were determined to obtain the desired properties of ZNPs based on particle size, polydispersity index and EE by using a central composite rotatable design. The nanoprecipitation method was more appropriate for producing chestnut and cedar shell/bark extract-loaded nanoparticles. In contrast, the high-speed homogenization method was suitable for producing sweetgum bark extract-loaded nanoparticles. As a result of the encapsulation of various shell/bark extracts within zein nanoparticles, value-added products were generated from wastes having bioactive compounds. The developed zein nanoparticles for each extract type would offer eco-friendly, simple and safe food processing and packaging systems.

Introduction

Nanotechnology is an expanding and innovative technology used for developing nanoparticles which are at the dimensions changing between 1 and 100 nm and can be in different shapes as spherical, tubular, or irregularly shaped (Nowack & Bucheli, 2007). The fabrication and application of nanoparticles have been widely carried out in diverse fields such as agricultural, nutritional, medicinal, and pharmaceutical areas (Nasrollahzadeh, Sajadi, Sajjadi & Issaabadi, 2019). Nanoparticles are widely used to encapsulate functional compounds, essential oils, antimicrobial agents and natural extracts to provide good stability, controlled delivery, improved efficacy, enhanced bioactivity and bioavailability (Lammari, Louaer, Meniai & Elaissari, 2020). High-energy and low-energy methods can be used to develop materials with nanoscale dimensions. High-pressure homogenization, ultrasonication and high-speed homogenization devices form nanoparticles using high-energy methods. These methods have the advantages of control size distribution, high efficiency and scalability. On the other hand, low-energy approaches such as spontaneous emulsification, ionotropic gelation and nanoprecipitation methods require low energy for the production of nanoparticles (Silva, Cerqueira & Vicente, 2012). Among these methods used for the production of nanoparticles, the nanoprecipitation method is known as the most straightforward and helpful method based on solvent displacement (Lammari et al., 2020). In the nanoprecipitation method, different strategies have been developed, such as covalent binding of the active substance to the biopolymer before the nanoparticle is prepared or to the surface of the nanoparticle afterwards, adsorption of the active substance to the biopolymeric carrier system, or entrapment of the active substance into the biopolymeric matrix while preparing the nanoparticle (Bal Öztürk, 2015). For instance, thymol-loaded chitosan nanoparticles added to chitosan-quinoa protein-based films (Medina et al., 2019), curcumin-loaded zein-caseinate-sodium alginate nanoparticles (Liu, Jing, Han, Zhang & Tian, 2019), silmarin loaded zein nanoparticles added to bacterial cellulose-based films (Tsai, Yang, Ho, Tsai & Mi, 2018) and zein nanoparticles added to whey-based films (Oymaci & Altinkaya, 2016) were obtained by using nanoprecipitation method. High-speed homogenization and high-pressure homogenization

* Corresponding author.
E-mail address: hilal.nadeem@adu.edu.tr (H.Ş. Nadeem).

https://doi.org/10.1016/j.fhfh.2023.100151
Received 6 May 2023; Received in revised form 4 August 2023; Accepted 10 August 2023
Available online 12 August 2023

methods are also widely applied in studies. However, in these methods, the energy produced from the devices can be dispersed in the environment, causing an increase in the sample's heat (Anton, Benoit & Saulnier, 2008).

Ultrasonication, the newest method among high-energy methods, is mainly used in enzyme inactivation, extraction, microorganism inhibition, homogenization and emulsification applications in the food industry (Yüksel, 2013). In recent years, nano-sized active compounds have been obtained by ultrasonication and are widely used to develop functional foods or food packaging. Boufi et al. (2018) studied starch nanoparticles obtained by ultrasonication, performed at 100% amplitude at different times (15, 30, 45, 60, 75, 90, and 105 min) and presented nanoparticles with decreasing sizes by increasing sonication time. In order to increase the bioactive properties of oregano (*Zataria multiflora*) essential oil, gum-based films containing nanoemulsions were obtained by applying high-intensity ultrasonication at different times (0, 2.5, 5, and 10 min). The antimicrobial effect of the films against *E. coli* and *B. cereus* microorganisms increased in parallel with the increase in ultrasonication time. The decrease in particle size, depending on the increasing time, also increased the antimicrobial effect of the nanoemulsion (Gahruie, Ziaee, Eskandari & Hosseini, 2017). To develop carotenoid-enriched nanoemulsion, starch nanoparticles with particle sizes smaller than 60 nm were obtained by combining ultrasonication and high-pressure homogenization techniques (Chutia & Mahanta, 2021).

Protein-based nanoparticles are gaining increasing interest as a carrier of bioactive compounds. Many advantages, including low toxicity, biodegradability, metabolizability, biocompatibility, stability, encapsulation ability and low price, make the protein-based nanoparticles more attractive (Lohcharoenkal, Wang, Chen & Rojanasakul, 2014; Pauluk, Padilha, Khalil & Mainardes, 2019). The ability of protein particles to provide the targeted functional properties depends on composition, size, morphology, charge and particle properties such as polarity (McClements, 2015). Zein is a significant protein naturally present in corn. It is preferred as an ideal material for encapsulating bioactive components because it is an alcohol-soluble and water-insoluble protein Zhang, Khan, Cheng and Liang (2019). Sodium caseinate is used as an electrosteric stabilizer in producing zein nanoparticles. It is a milk protein widely used in the food industry as an emulsifier and stabilizer (Ahmed, Hosny, Al-Sawahli & Fahmy, 2015). Thus, zein and sodium caseinate are blended to produce nanoparticles which encapsulate the bioactive compounds.

Plant-based extracts, which are rich in antioxidants and antimicrobial compounds, play a role in increasing the shelf life of foods. Regarding the source of plant-based extracts, fruit shells and bark from trees offer a cost-effective alternative source. In the previous study, chestnut shells, which are a high amount of waste from chestnut processing, cedar bark derived from cuts in the forest, and sweetgum tree bark as a pressing waste of sweetgum oil, were chosen as rich and cost-free sources of bioactive compounds. Chestnut, cedar and sweetgum shell/bark extracts were obtained under optimum conditions by analyzing the bioactive properties of the extracts (Erdoğdu, 2021). However, the practical use of the extracts while preserving and boosting their bioactive properties can be possible by encapsulating them into nanoparticle structures.

Cedar and sweetgum have been the subject of many studies in forestry. Furthermore, there are studies in which the extracts obtained from different parts of the cedar and sweetgum tree indicated antioxidant and antimicrobial properties. In terms of the phenolic compounds, a significant amount (27.7 mg cyanidin equivalent/g) of tannins was found in water-based extracts obtained from Taurus cedar bark (Gönültaş & Sarıalan, 2017). Essential oils obtained by hexane extraction from cedar tree leaves showed antimicrobial activity against Gram-positive and Gram-negative bacteria. It has been reported to inhibit the growth of *Escherichia coli, Pseudomonas aeroginosa, Klebsiella pneumoniae, Staphylococcus aureus, Staphylococcus intermedius, Enterococcus faecalis*, and *Bacillus sphericus* microorganisms at different minimum inhibition concentrations (Derwich, Benziane & Boukir, 2010). There are some studies in which the properties of sweetgum leaves, bark and oil are determined and used as a natural preservative in herbal treatments. The shelf life of seabass fish immersed in sweetgum leaf extract (0.1%, 0.5 and 1% solutions) was extended by 3 days at 4 °C, and the protective effect increased as the concentration of the extract increased. As a result of the sensory analysis performed in the study, it was observed that the control group decreased below the consumable limits after day 15 of storage. In contrast, the groups treated with leaf extract were acceptable until the 18th day of storage (Yapıcı, Baygar, Metin & Alparslan, 2015). While 55% of chestnuts produced worldwide are consumed fresh, 45% are offered to the market as a processed product. Chestnut fruit attracts attention with its brown peel, which has functional compounds. Chestnut shell is a valuable food by-product with its high phenolic content and antioxidant properties (Kasımoğlu, Yıldırım, Alkan, Topuz & Nadeem, 2016). The phenolic compound found in the highest amount, with 13.2% in the chestnut shell, was pyrogallol (Gullón et al., 2018). Squillaci et al. (2018) used environmentally friendly methods to obtain bioactive compounds from chestnut shell; extracts rich in gallic acid, protocatechuic acid and ellagic acid were obtained from inner and outer chestnut shells with water at a rate of 5% (w/v). Phenolic compounds such as gallic acid and ellagic acid found in chestnut shell are well known for their antioxidant and anticancer properties. The natural antioxidant properties of chestnut shell extracts were compared with the butyl hydroxytoluene (BHT) as a synthetic antioxidant and ascorbic acid (AA) as a natural antioxidant, the free radical scavenging activity (44%) of the inner and outer chestnut shell extracts were found to be much more potent compared to activities of BHT and AA (7.2% and 29%) (Squillaci et al., 2018).

So far, there has been little research to help literature on making protein-based nanoparticles, including shell/bark waste extract. Besides that, limited studies have been found on evaluating the different methods and formulations used in producing ZNPs. This study aimed to obtain chestnut, cedar, and sweetgum shell/bark waste extract-loaded ZNPs and investigate the effects of different production methods and different formulations on the properties of ZNPs.

Materials and methods

Materials

Sodium caseinate from milk and zein from maize were purchased from GMT Food (İstanbul, Turkey) and Sigma-Aldrich (St. Louis, MO, USA), respectively. Optimum shell/bark extracts of chestnut, cedar and sweetgum were obtained from the previous study based on optimizing extraction conditions (Erdoğdu, 2021). HPLC-grade acetonitrile and glacial acetic acid were bought from ISOLAB (Eschau, Germany) and Merck (Darmstadt, Germany), respectively. All other chemicals were of analytical grade.

Production of nanoparticles

Sodium caseinate was dissolved in water at 1% (w/v) concentration, and zein was dissolved in 80% (v/v) ethanol at a defined concentration (mg/mL). Shell/bark waste extracts were added to the zein solution at a defined concentration (mg/mL). ZNPs were prepared based on three different methods. In the nanoprecipitation method, zein solution was dropwise to an equal amount of sodium caseinate solution under continuous stirring in a magnetic stirrer. In the high-speed homogenization method, zein solution was mixed with an equal amount of sodium caseinate solution under continuous mixing in a homogenizer (Ultra Turrax IKA, T18). Zein solution was mixed with an equal amount of sodium caseinate solution, and immediately ultrasonic waves were applied at ambient temperature to prepare ZNPs by ultrasonic homogenizer (Hielscher, UP400ST).

Experimental design

In order to determine the effects of the production method and process conditions on the physical and chemical properties of ZNPs, a central composite rotatable design (CCRD) was used. The design included 30 runs for each nanoparticle formation method (3 methods x 3 extracts x 30 different conditions = 270 total trials), with six runs at the central point. Independent variables and their levels are represented in Table 1. At the same time, the range of zein concentration (mg/ml, X1) and extract ratio (mg/ml, X4) were the same terms for all nanoparticle production methods. Independent variables were flow rate (ml/s, X5) and mixing speed (rpm, X6) for the nanoprecipitation method, homogenization rate (rpm, X3) and time (min, X2) for high-speed homogenization method and amplitude (%, X7) and time (min, X2) for ultrasonic homogenization method. Nanoparticle production was carried out according to the CCRD experimental design (Table 2), and all analyses were performed in three replicates. The results were given as the mean value with the standard deviation.

Particle size, polydispersity index, transmittance and zeta(ζ)-potential

Particle size, polydispersity index (PDI), transmittance and zeta potential analyses of nanoparticles were obtained using the Litesizer™ 500 instrument (Anton Paar GmbH, Graz, Austria). The particle size is reported as the mean hydrodynamic diameter (nm). PDI and transmittance mean values were given as a percentage (%). The mean zeta potential values of the particles were presented as mV. All measurements were carried out at 25 °C.

Encapsulation efficiency

In order to determine the encapsulation efficiency (EE) of ZNPs containing chestnut, cedar and sweetgum extracts, it was aimed to determine the dominant phenolic substance in each extract by high-performance liquid chromatography (HPLC) analysis. Each extract was mixed with 80% ethanol at a ratio of 1:10 and kept in a water bath at 60 °C for 1 hour to extract phenolic compounds. It was then passed through a 0.45 μm filter and analyzed in HPLC. Gradient elution was performed for 65 min at a flow rate of 0.8 mL/min and a colon temperature of 30 °C by using the following steps of solvents A [2% glacial acetic acid)] and B (70% acetonitrile): 95:5 (A:B) for 2 min, 60:40 for 10 min, 45:55 for 20 min, 40:60 for 25 min, 25:75 for 35 min, 20:80 for 60 min, 95:5 for 65 min. UV detection was performed at 280, 320 and 360 nm wavelengths, and phenolic compounds were identified by comparing the chromatographic retention times with standard solutions of phenolics.

Like extract, phenolic compounds were extracted by mixing the nanoparticles with 80% ethanol at a ratio of 1:1 and keeping them in a water bath at 60 °C for 1 hour. Then, the extract of ZNPs passed through a 0.45 μm filter and was analyzed in HPLC using the same method. Encapsulation efficiency calculations were performed according to Li et al. (2018) regarding the selected phenolic compound. The equation used to calculate encapsulation efficiency (%) is below.

$$EE\,(\%) = M/M_0 \times 100$$

M: the concentration (ppm) of encapsulated phenolic compound in the nanoparticle solution

M_0: the concentration (ppm) at which the encapsulated phenolic compound was added to the solution

Statistical evaluation

The effects of independent process variables on responses for each nanoprecipitation, high-speed homogenization and ultrasonic homogenization methods were modelled by regression analysis using the Design Expert 7.0 software based on central composite rotatable design (CCRD).

Transmission electron microscopy (TEM)

Nanoemulsions have increased attention in being a vehicle for carrying functional compounds and protecting the desired compound. Nanocomposite active packaging films are the focus of the present study. In another study (unpublished data), active nanocomposite films based on pectin and gelatin were developed by incorporating nanoparticles obtained in optimum methods and conditions into the composite film structure. Transmission electron microscopy (TEM) analysis of those bionanocomposite films were carried out. Light field imaging was performed under 120 kV voltage using a lanthanum hexaboride (LaB6) electron gun TEM device.

Results and discussion

The results of physical and chemical properties of the chestnut shell, cedar and sweetgum bark waste extract-loaded ZNPs produced by nanoprecipitation, high homogenization speed and ultrasonic homogenization methods were presented in Table 3, Tables 4 and 5, respectively. ANOVA results for particle size, PDI and encapsulation efficiency of nanoparticles produced by nanoprecipitation, high homogenization speed and ultrasonic homogenization methods were given in Table 6.

Particle size

Particle size is one of the most important parameters used to characterize nanoparticles. It can dramatically affect the absorption and distribution of nanoparticles in nutritional and medical applications. The main parameters that influence nanoparticles' stability and directly affect core material's functional activity are properties of nanoparticles, primarily particle size, PDI and zeta potential. Because of this reason,

Table 1
Independent variables and their levels for Central Composite Rotatable Design (CCRD).

		Coded values				
Nanoparticle production method	Independent variables	−2	−1	0	1	2
Nanoprecipitation	X_1. Zein concentration (mg/ml)	5.0	7.5	10.0	12.5	15.0
	X_6. Mixing speed (rpm)	500	750	1000	1250	1500
	X_5. Flow rate (ml/s)	1.0	1.2	1.4	1.6	1.8
	X_4. Extract ratio (mg/ml)	2.0	3.5	5.0	6.5	8.0
High speed homogenization	X_1. Zein concentration (mg/ml)	5.0	7.5	10.0	12.5	15.0
	X_3. Homogenization rate (rpm)	3000	4750	6000	8250	10,000
	X_2. Time (min)	3	4	5	6	7
	X_4. Extract ratio (mg/ml)	2.0	3.5	5.0	6.5	8.0
Ultrasonic homogenization	X_1. Zein concentration (mg/ml)	5.0	7.5	10.0	12.5	15.0
	X_7. Amplitude (%)	20	25	30	35	40
	X_2. Time (min)	1	2	3	4	5
	X_4. Extract ratio (mg/ml)	2.0	3.5	5.0	6.5	8.0

Table 2
CCRD experimental design.

			Nanoprecipitation		High speed homogenization		Ultrasonic homogenization	
Exp.	X_1 (mg/ml)	X_4 (mg/ml)	X_5 (ml/s)	X_6 (rpm)	X_2 (min)	X_3 (rpm)	X_2 (min)	X_7 (%)
1	7,50	3,50	1,20	750	4	4750	2	25
2	12,5	3,50	1,20	750	4	4750	2	25
3	7,50	3,50	1,20	1250	4	8250	2	35
4	12,5	3,50	1,20	1250	4	8250	2	35
5	7,50	3,50	1,60	750	6	4750	4	25
6	12,5	3,50	1,60	750	6	4750	4	25
7	7,50	3,50	1,60	1250	6	8250	4	35
8	12,5	3,50	1,60	1250	6	8250	4	35
9	7,50	6,50	1,20	750	4	4750	2	25
10	12,5	6,50	1,20	750	4	4750	2	25
11	7,50	6,50	1,20	1250	4	8250	2	35
12	12,5	6,50	1,20	1250	4	8250	2	35
13	7,50	6,50	1,60	750	6	4750	4	25
14	12,5	6,50	1,60	750	6	4750	4	25
15	7,50	6,50	1,60	1250	6	8250	4	35
16	12,5	6,50	1,60	1250	6	8250	4	35
17	5,00	5,00	1,40	1000	5	6500	3	30
18	15,0	5,00	1,40	1000	5	6500	3	30
19	10,0	5,00	1,40	500	5	3000	3	20
20	10,0	5,00	1,40	1500	5	10,000	3	40
21	10,0	5,00	1,00	1000	3	6500	1	30
22	10,0	5,00	1,80	1000	7	6500	5	30
23	10,0	2,00	1,40	1000	5	6500	3	30
24	10,0	8,00	1,40	1000	5	6500	3	30
25	10,0	5,00	1,40	1000	5	6500	3	30
26	10,0	5,00	1,40	1000	5	6500	3	30
27	10,0	5,00	1,40	1000	5	6500	3	30
28	10,0	5,00	1,40	1000	5	6500	3	30
29	10,0	5,00	1,40	1000	5	6500	3	30
30	10,0	5,00	1,40	1000	5	6500	3	30

their stability must be considered before they are implemented in the food and pharmaceutical industry. The effects of different production methods and process conditions on the particle size of ZNPs loaded with shell/bark waste extracts were investigated.

The particle size of nanoparticles produced by the nanoprecipitation method using chestnut, cedar and sweetgum shell/bark extracts varied between 143.47 and 187.23 nm (Table 3), 136.27 and 202.40 nm (Table 4), and 132.81 and 178.87 nm (Table 5), respectively. The ANOVA results (Table 6) showed that the zein concentration and extract ratio were the significant parameters affecting the particle size ($p < 0.05$) of the nanoparticles loaded with chestnut shell extract. As seen in Fig. 1a, the particle size was the highest value at maximum and minimum levels of the zein concentration. With the increase in zein concentration, the size of the nanoparticles decreased up to a specific value but increased after a particular value. The reduction in the size of nanoparticles may be due to the electrostatic interaction between zein, sodium caseinate and extract. The increase in particle diameter with the increase of zein concentration after a specific value may be due to the formation of self-assembled nanospheres. Liang et al. (2017) investigated the effect of zein concentration on nanoparticle diameter. They reported that as the zein concentration increased from 72 to 216 mg, the average particle diameter of the nanoparticles decreased from 240.6 to 197.6 nm. However, a further increase in zein concentration (288 mg) increased the particle size (205.5 nm). Perturbation plots (Fig. 1) showed that regardless of extract type, the particle size of the NPs increased with the extract ratio, whereas a small amount of change in particle size was observed with the mixing rate. The effect of the extract ratio can be interpreted as the accumulation of extract molecules on the zein particle's surface and preventing caseinate absorption, thus increasing the hydrophobic interaction between the nanoparticles, which leads to aggregation and, consequently, the increase in particle size. It was observed that the particle size of nanoparticles containing cedar bark extract was affected by the zein concentration, flow rate and extract ratio. The particle diameter increased with the increase of all three independent process variables. In nanoparticles containing sweetgum bark extract, the increase in zein concentration and flow rate led to an increase in particle size.

In this study, the core and shell of nanoparticles consist of a hydrophobic protein zein and an amphiphilic protein caseinate, respectively. When the zein solution is injected into the caseinate solution, the ethanol surrounding the zein particles begins to diffuse into the antisolvent phase. The local ethanol concentration exceeds the dissolution limit (Zhong, Jin, Xiao, Tian & Zhang, 2008). This situation causes the environment's zein molecules to coalesce, thus to protein precipitation. This precipitation can be prevented by using caseinate in an aqueous solution. Caseinate both surrounds the exposed non-polar regions in the medium and adsorbs on the surface of the zein colloidal particles. Caseinate plays a vital role in developing aggregation stability or preventing the precipitation of zein particles. It can treat as a stabilizer by increasing electrostatic and steric impulsion between the zein particles, thereby stabilizing colloidal particles of zein.

Moreover, the mass ratio of zein to sodium caseinate was an important parameter affecting the size of ZNPs. The stability of the obtained suspensions decreases with the increase of this ratio. The reason is that the surfaces of colloidal ZNPs are not sufficiently saturated with sodium caseinate (Liu et al., 2019). As seen in Fig. 1b and c, there was an increase in the mean particle diameter of the nanoparticles produced using cedar and sweetgum bark extracts with increasing zein concentration in the solvent phase. ZNPs with small particle sizes at low zein concentrations can be explained by the effect of caseinate on saturation, nucleation and growth periods. As stated above, if the amount of caseinate in the antisolvent phase is insufficient, it cannot surround all the zein particles formed and may cause flocculation (Guzey & McClements, 2006). However, the high initial protein ratio in the solvent phase leads to an increase in the concentration of the suspension. As particles' collision probability increases with increasing concentration, aggregation is likely to occur (Joye & McClements, 2013). In addition, since high protein concentration caused the viscosity of the suspension to increase, it may have prevented the homogeneous mixing of the solvent and anti-solvent in the system (Ebert, Koo, Weiss & McClements,

Table 3
Physical and chemical properties of chestnut shell extract loaded ZNPs produced by nanoprecipitation, high homogenization speed and ultrasonic homogenization methods.

Exp.	Chestnut shell extract loaded ZNPs by nanoprecipitation					Chestnut shell extract loaded ZNPs by high homogenization speed					Chestnut shell extract loaded ZNPs by ultrasonic homogenization				
	Particle size (nm)	PDI (%)	Transmittance	Zeta potential (mV)	EE (%)	Particle size (nm)	PDI (%)	Transmittance	Zeta potential (mV)	EE (%)	Particle size (nm)	PDI (%)	Transmittance	Zeta potential (mV)	EE (%)
1	160.50 ±0.07	0.15 ±0.00	73.47±0.03	35.98±0.03	82.18 ±0.17	181.49 ±0.24	0.08 ±0.01	53.47±0.39	38.80±0.14	83.79 ±0.07	161.60 ±0.54	0.14 ±0.00	71.85±0.07	36.60±0.14	82.85 ±0.56
2	156.36 ±0.04	0.09 ±0.00	57.60±0.00	37.48±0.53	89.81 ±2.10	207.50 ±0.11	0.10 ±0.00	33.32±0.11	39.80±0.00	95.11 ±1.00	197.86 ±0.15	0.12 ±0.01	32.85±0.07	40.00±0.14	95..00 ±0.11
3	162.28 ±0.16	0.15 ±0.02	73.17±0.18	39.10±0.53	84.27 ±0.05	201.62 ±0.60	0.15 ±0.01	45.30±0.14	38.02±0.03	83.37 ±0.10	156.56 ±0.19	0.11 ±0.00	69.00±0.00	36.72±0.03	82.91 ±0.15
4	151.62 ±0.37	0.12 ±0.02	59.30±0.00	38.15±0.07	96.83 ±0.31	249.65 ±1.77	0.14 ±0.01	10.87±0.03	39.35±0.07	95.76 ±0.34	201.85 ±0.07	0.13 ±0.00	31.87±0.03	37.55±0.07	94.36 ±0.07
5	149.51 ±0.25	0.16 ±0.01	64.30±0.99	38.65±0.07	83.98 ±0.13	180.55 ±0.17	0.09 ±0.01	52.70±0.00	40.10±0.00	83.89 ±0.14	169.89 ±0.11	0.10 ±0.01	64.02±0.03	36.45±0.21	83.20 ±0.12
6	161.54 ±0.04	0.08 ±0.00	55.80±0.14	38.20±0.14	93.34 ±2.07	217.17 ±0.74	0.09 ±0.00	24.92±0.03	39.07±0.11	96.00 ±0.56	217.80 ±0.00	0.12 ±0.00	23.80±0.00	37.35±0.21	94.53 ±0.10
7	165.49 ±0.21	0.18 ±0.03	71.40±0.14	37.80±0.14	84.41 ±0.33	203.47 ±0.39	0.10 ±0.01	47.30±0.00	40.45±0.07	83.86 ±0.06	171.71 ±0.16	0.10 ±0.00	61.00±0.00	37.30±0.14	83.06 ±0.08
8	161.57 ±0.15	0.10 ±0.02	54.30±0.42	35.10±0.14	94.35 ±0.55	254.75 ±0.21	0.10 ±0.01	12.23±0.07	39.10±0.00	96.11 ±0.27	232.45 ±0.64	0.15 ±0.01	15.37±0.03	38.30±0.14	95.00 ±0.05
9	176.47 ±0.16	0.24 ±0.00	34.40±0.71	38.33±0.03	45.18 ±0.31	211.10 ±0.00	0.26 ±0.00	20.85±0.07	37.05±0.07	45.19 ±0.17	178.52 ±0.21	0.17 ±0.01	44.72±0.03	40.97±0.03	44.70 ±0.07
10	158.40 ±0.40	0.09 ±0.00	55.00±0.28	36.15±0.21	48.93 ±0.65	186.89 ±0.07	0.12 ±0.00	31.57±0.11	40.10±0.14	51.17 ±0.07	196.80 ±0.12	0.08 ±0.02	38.17±0.14	36.80±0.00	51.28 ±0.26
11	158.58 ±0.50	0.24 ±0.00	40.60±0.00	38.40±0.00	44.86 ±0.09	205.62 ±0.11	0.23 ±0.00	24.22±0.18	39.10±0.14	44.99 ±0.06	175.47 ±0.37	0.22 ±0.00	40.30±0.00	36.90±0.00	44.52 ±0.20
12	152.43 ±0.09	0.10 ±0.00	57.45±0.07	37.20±0.28	52.38 ±0.14	232.30 ±0.00	0.11 ±0.01	13.30±0.00	38.67±0.11	51.25 ±0.17	191.17 ±0.23	0.08 ±0.01	40.30±0.00	36.25±0.07	50.71 ±0.46
13	169.43 ±0.04	0.24 ±0.00	40.37±0.03	42.75±0.07	44.67 ±0.08	208.35 ±0.49	0.26 ±0.01	26.20±0.28	37.77±0.18	44.85 ±0.23	185.41 ±0.24	0.20 ±0.01	35.60±0.42	39.60±0.14	44.85 ±0.77
14	160.66 ±0.16	0.12 ±0.00	52.50±0.42	37.70±0.00	51.62 ±0.08	194.14 ±0.17	0.14 ±0.05	25.40±0.00	40.30±0.14	51.27 ±0.23	189.52 ±0.57	0.11 ±0.00	41.80±0.00	35.65±0.07	47.47 ±0.77
15	173.45 ±0.18	0.24 ±0.00	40.25±0.07	39.57±0.03	44.64 ±0.04	220.95 ±0.46	0.25 ±0.00	16.75±0.07	39.70±0.00	45.10 ±0.03	175.55 ±0.33	0.20 ±0.00	40.57±0.03	37.60±0.00	44.97 ±0.07
16	168.11 ±0.06	0.15 ±0.00	49.25±0.03	35.25±0.07	52.10 ±0.20	240.30 ±0.14	0.12 ±0.00	12.35±0.07	35.52±0.03	51.24 ±0.07	202.52 ±0.03	0.11 ±0.00	35.37±0.03	33.25±0.07	50.76 ±0.14
17	187.22 ±0.09	0.26 ±0.00	52.25±0.07	40.43±0.03	67.19 ±1.97	213.50 ±0.00	0.25 ±0.00	29.70±0.28	42.30±0.14	54.24 ±0.07	176.03 ±0.09	0.23 ±0.01	49.37±0.03	37.40±0.28	57.45 ±0.03
18	170.32 ±0.16	0.09 ±0.00	47.10±0.00	36.35±0.07	68.95 ±0.59	244.25 ±0.64	0.16 ±0.01	10.52±0.03	38.20±0.14	70.81 ±0.31	215.32 ±0.32	0.10 ±0.03	22.20±0.00	33.72±0.03	66.87 ±1.79
19	159.38 ±0.06	0.11 ±0.00	62.05±0.07	38.75±0.07	61.81 ±0.85	174.08 ±0.63	0.17 ±0.00	37.80±0.00	38.37±0.03	60.02 ±0.00	173.06 ±0.00	0.10 ±0.00	57.30±0.00	35.90±0.07	58.36 ±0.56
20	151.15 ±0.17	0.15 ±0.00	72.27±0.11	36.20±0.57	61.82 ±0.14	216.35 ±0.21	0.19 ±0.00	29.20±0.14	39.45±0.49	62.25 ±0.66	199.37 ±0.02	0.15 ±0.00	43.35±0.21	35.80±0.00	57.80 ±1.77
21	145.45 ±0.10	0.12 ±0.01	71.40±0.57	34.00±0.00	62.31 ±0.14	186.32 ±0.78	0.16 ±0.00	36.56±0.09	37.02±0.03	61.13 ±1.11	180.76 ±0.16	0.11 ±0.00	48.45±0.07	36.90±0.11	58.56 ±0.49
22	150.19 ±0.63	0.13 ±0.00	69.02±0.03	36.30±0.14	62.14 ±0.04	196.66 ±0.30	0.18 ±0.02	32.70±0.14	41.05±0.07	67.74 ±1.05	203.55 ±0.35	0.10 ±0.00	34.70±0.07	36.50±0.14	59.17 ±1.90
23	152.21 ±0.10	0.08 ±0.01	64.32±0.11	37.70±0.14	–	195.46 ±0.53	0.06 ±0.00	45.00±0.21	35.57±0.25	–	199.03 ±0.01	0.11 ±0.00	36.30±0.00	36.10±0.00	–
24	157.16 ±0.48	0.20 ±0.00	39.50±0.14	37.15±0.21	38.90 ±0.02	197.02 ±0.01	0.21 ±0.00	19.85±0.07	37.00±0.00	39.46 ±1.30	196.50 ±0.43	0.14 ±0.00	27.10±0.00	38.15±0.21	39.18 ±0.15
25	148.66 ±0.04	0.09 ±0.00	63.40±0.14	36.25±0.00	62.57 ±0.24	174.13 ±0.09	0.14 ±0.00	53.10±0.14	29.50±0.14	62.97 ±1.41	198.98 ±0.00	0.14 ±0.01	42.40±0.00	35.50±0.42	62.40 ±0.27
26	152.94 ±0.05	0.12 ±0.01	70.73±0.07	35.25±0.35	62.22 ±0.10	169.36 ±1.70	0.11 ±0.01	53.87±0.03	29.40±0.21	63.18 ±0.07	194.63 ±0.02	0.13 ±0.03	44.60±0.28	35.67±0.07	63.52 ±0.14
27	150.97 ±0.00	0.14 ±0.00	67.65±0.21	35.70±0.28	62.47 ±0.11	185.62 ±0.08	0.14 ±0.00	53.57±0.46	29.85±0.07	63.51 ±0.11	201.35 ±0.49	0.10 ±0.01	39.50±0.00	36.37±0.03	62.46 ±0.13
28	143.46 ±0.54	0.11 ±0.00	64.97±0.03	36.55±0.21	62.29 ±0.24	171.70 ±0.10	0.12 ±0.00	48.80±0.00	31.55±0.07	64.42 ±7.16	190.56 ±0.32	0.13 ±0.00	48.60±0.14	34.05±0.07	63.07 ±0.33
29	148.22 ±0.01	0.09 ±0.01	64.25±0.21	35.60±0.28	62.48 ±0.10	180.78 ±0.79	0.16 ±0.01	40.25±0.78	30.40±0.00	62.42 ±0.34	186.72 ±0.28	0.13 ±0.00	46.80±0.07	34.32±0.39	62.41 ±0.19
30	148.64 ±0.17	0.09 ±0.00	62.30±0.14	34.60±0.28	62.27 ±0.13	175.48 ±0.09	0.16 ±0.00	44.47±0.03	32.55±0.07	61.64 ±1.39	190.17 ±0.14	0.09 ±0.00	43.85±0.07	34.25±0.49	61.69 ±0.40

Table 4
Physical and chemical properties of Toros cedar bark extract loaded ZNPs produced by nanoprecipitation, high homogenization speed and ultrasonic homogenization methods.

	Toros cedar bark extract loaded ZNPs by nanoprecipitation					Toros cedar bark extract loaded ZNPs by high homogenization speed					Toros cedar bark extract loaded ZNPs by ultrasonic homogenization				
Exp.	Particle size (nm)	PDI (%)	Transmittance	Zeta potential (mV)	EE (%)	Particle size (nm)	PDI (%)	Transmittance	Zeta potential (mV)	EE (%)	Particle size (nm)	PDI (%)	Transmittance	Zeta potential (mV)	EE (%)
1	146.54 ±0.24	0.08 ±0.00	72.35±0.35	30.40±0.57	78.58 ± 0.11	155.76 ±0.25	0.14 ±0.00	66.77±0.03	32.75±0.21	78.59 ± 0.04	182.83 ±0.17	0.12 ±0.00	55.70±0.00	27.62±0.11	78.11 ± 0.04
2	160.01 ±0.09	0.05 ±0.00	50.25±0.21	30.32±0.18	78.99 ± 0.10	198.66 ±0.04	0.17 ±0.00	24.20±0.00	32.50±0.00	79.21 ± 0.07	218.15 ±0.21	0.16 ±0.00	14.75±0.07	29.40±0.00	78.83 ± 0.42
3	141.50 ±0.59	0.11 ±0.00	73.45±0.07	29.25±0.21	78.32 ± 0.14	164.53 ±0.42	0.11 ±0.00	48.75±0.21	32.20±0.00	78.61 ± 0.05	179.24 ±0.04	0.13 ±0.01	56.57±0.03	28.65±0.21	78.47 ± 0.10
4	158.13 ±0.21	0.10 ±0.01	53.10±0.14	32.32±0.32	78.99 ± 0.27	333.54 ±0.55	0.25 ±0.00	0.70±0.00	36.60±0.14	79.67 ± 0.15	259.15 ±0.92	0.15 ±0.00	7.60±0.00	31.82±0.60	78.84 ± 0.25
5	142.48 ±0.07	0.13 ±0.03	75.15±0.21	31.20±0.00	78.47 ± 0.08	155.61 ±0.31	0.15 ±0.00	61.37±0.11	33.50±0.28	78.54 ± 0.02	188.15 ±0.04	0.08 ±0.00	53.70±0.00	28.22±0.18	78.15 ± 0.04
6	172.31 ±0.00	0.09 ±0.00	47.45±0.21	31.25±0.07	79.17 ± 0.05	215.45 ±0.21	0.20 ±0.01	9.30±0.28	34.20±0.28	79.28 ± 0.03	240.65 ±0.49	0.12 ±0.00	10.40±0.00	30.65±0.64	78.28 ± 0.18
7	140.36 ±0.07	0.15 ±0.00	73.15±0.07	33.70±0.14	78.31 ± 0.15	180.26 ±0.23	0.15 ±0.00	46.55±0.07	32.45±0.49	78.53 ± 0.18	195.67 ±0.29	0.12 ±0.01	48.10±0.00	29.50±0.00	77.84 ± 0.1
8	164.77 ±0.29	0.07 ±0.00	50.22±0.95	32.30±0.28	79.15 ± 0.18	430.25 ±0.21	0.27 ±0.00	2.30±0.00	36.55±0.21	79.26 ± 0.11	300.60 ±0.00	0.19 ±0.01	2.80±0.00	32.72±0.11	78.52 ± 0.14
9	152.37 ±0.25	0.05 ±0.01	66.15±0.49	32.65±0.07	42.69 ± 0.04	168.72 ±0.17	0.14 ±0.00	64.70±0.00	28.55±0.07	42.37 ± 0.10	182.55 ±0.00	0.11 ±0.02	54.77±0.03	28.60±0.28	42.00 ± 0.01
10	176.77 ±0.30	0.03 ±0.01	44.25±0.07	33.60±0.14	42.82 ± 0.01	227.87 ±0.46	0.14 ±0.00	11.50±0.00	31.55±0.49	42.72 ± 0.25	231.45 ±0.21	0.14 ±0.00	12.48±0.08	31.30±0.00	42.37 ± 0.12
11	157.22 ±0.32	0.10 ±0.00	70.35±0.07	30.80±0.14	42.31 ± 0.02	187.52 ±0.54	0.13 ±0.00	43.05±0.07	35.05±0.07	42.64 ± 0.01	169.13 ±0.42	0.13 ±0.00	63.12±0.26	27.65±0.21	41.76 ± 0.07
12	181.65 ±0.35	0.09 ±0.01	43.80±0.00	29.70±0.14	42.66 ± 0.19	366.52 ±0.32	0.26 ±0.00	0.20±0.00	36.30±0.00	42.99 ± 0.14	205.00 ±0.14	0.11 ±0.01	24.05±0.10	28.70±0.00	41.93 ± 0.02
13	153.69 ±0.28	0.12 ±0.00	68.10±0.00	29.25±0.21	42.32 ± 0.02	172.56 ±0.26	0.14 ±0.00	56.70±0.28	31.92±0.03	42.53 ± 0.06	166.73 ±0.25	0.09 ±0.00	64.37±0.03	26.77±0.03	41.84 ± 0.25
14	193.63 ±0.26	0.05 ±0.00	39.35±0.07	28.62±0.11	42.63 ± 0.02	224.40 ±0.14	0.19 ±0.00	8.90±0.00	32.45±0.07	42.96 ± 0.06	208.87 ±0.39	0.13 ±0.00	21.57±0.05	28.20±0.00	42.19 ± 0.25
15	157.66 ±0.22	0.10 ±0.01	67.02±0.03	29.95±0.07	42.51 ± 0.02	190.39 ±0.02	0.18 ±0.01	41.80±0.00	32.25±0.21	42.63 ± 0.10	176.88 ±0.15	0.12 ±0.00	58.02±0.11	27.15±0.07	41.88 ± 0.08
16	202.40 ±0.21	0.07 ±0.00	35.10±0.00	29.70±0.14	42.65 ± 0.18	428.22 ±0.75	0.25 ±0.00	0.30±0.00	36.60±0.28	42.35 ± 0.03	230.10 ±0.49	0.19 ±0.01	14.00±0.00	30.20±0.00	42.10 ± 0.05
17	140.52 ±0.00	0.15 ±0.00	79.10±0.00	26.45±0.35	54.9 ± 0.04	157.16 ±0.11	0.13 ±0.00	77.45±0.21	33.20±0.00	54.95 ± 0.01	153.61 ±0.09	0.11 ±0.00	80.17±0.34	23.25±0.21	54.40 ± 0.06
18	196.80 ±0.51	0.07 ±0.01	29.40±0.00	29.25±0.07	55.48 ± 0.4	386.05 ±1.34	0.26 ±0.00	0.40±0.00	35.47±0.03	56.07 ± 0.07	257.40 ±0.28	0.18 ±0.00	5.95±0.06	28.22±0.03	55.64 ± 0.26
19	191.72 ±0.25	0.07 ±0.02	45.20±0.21	30.40±0.14	55.27 ± 0.09	183.97 ±0.91	0.11 ±0.01	41.55±0.49	32.57±0.00	55.32 ± 0.07	197.67 ±0.49	0.11 ±0.00	40.92±0.03	26.62±0.03	55.03 ± 0.06
20	172.54 ±0.00	0.10 ±0.01	53.63±0.07	29.40±0.00	55.17 ± 0.07	354.80 ±0.00	0.22 ±0.01	0.60±0.00	39.40±0.28	55.51 ± 0.16	208.55 ±0.07	0.14 ±0.01	32.17±0.27	27.25±0.07	55.00 ± 0.03
21	136.27 ±0.17	0.06 ±0.01	70.22±0.25	27.00±0.00	55.15 ± 0.04	191.32 ±0.28	0.16 ±0.00	36.20±0.00	30.40±0.14	55.68 ± 0.05	200.05 ±0.07	0.13 ±0.01	40.00±0.00	30.40±0.14	54.71 ± 0.27
22	146.46 ±0.51	0.11 ±0.00	66.50±0.00	28.45±0.64	55.03 ± 0.04	225.60 ±0.32	0.22 ±0.01	9.93±0.03	33.45±0.21	55.57 ± 0.05	227.32 ±0.32	0.12 ±0.01	21.70±0.14	29.60±0.28	54.37 ± 0.07
23	152.32 ±0.22	0.12 ±0.00	63.50±0.00	29.40±0.14	–	211.93 ±0.25	0.22 ±0.03	23.35±0.21	30.40±0.42	–	231.65 ±0.21	0.15 ±0.01	27.78±0.08	29.95±0.78	–
24	158.03 ±0.18	0.11 ±0.00	58.85±0.07	29.67±0.03	34.61 ± 0.03	193.50 ±0.18	0.21 ±0.02	30.20±0.00	32.20±0.14	35.10 ± 0.17	206.75 ±1.34	0.13 ±0.00	30.00±0.00	30.37±0.25	34.03 ± 0.05
25	145.67 ±0.11	0.13 ±0.00	63.35±0.21	30.30±0.42	55.13 ± 0.07	207.60 ±0.71	0.21 ±0.02	20.45±0.07	30.53±0.25	55.81 ± 0.25	213.60 ±0.32	0.16 ±0.00	29.13±0.14	29.10±0.00	55.27 ± 0.03
26	150.50 ±0.05	0.09 ±0.00	62.43±0.03	26.70±0.00	55.06 ± 0.02	213.20 ±0.57	0.22 ±0.00	19.52±0.60	31.73±0.07	55.51 ± 0.14	208.35 ±0.35	0.15 ±0.00	33.40±0.00	31.40±0.00	54.95 ± 0.14
27	158.44 ±0.08	0.09 ±0.00	59.65±0.07	27.50±0.00	55.16 ± 0.11	205.40 ±0.28	0.18 ±0.01	26.10±0.00	30.83±0.07	55.57 ± 0.13	218.60 ±0.28	0.16 ±0.01	24.90±0.00	30.45±0.21	55.29 ± 0.07
28	149.60 ±0.20	0.11 ±0.01	61.50±0.14	28.22±0.11	55.19 ± 0.07	194.85 ±0.15	0.19 ±0.01	34.40±0.00	30.25±0.07	55.65 ± 0.05	217.97 ±0.11	0.17 ±0.00	25.50±0.00	31.30±0.00	55.13 ± 0.10
29	155.71 ±0.47	0.08 ±0.00	58.53±0.14	29.60±0.28	55.08 ± 0.11	192.51 ±0.03	0.16 ±0.02	35.15±0.07	29.57±0.14	55.23 ± 0.04	209.27 ±0.11	0.14 ±0.00	29.10±0.00	30.70±0.00	55.36 ± 0.10
30	155.27 ±0.16	0.09 ±0.01	60.80±0.00	31.35±0.07	55.17 ± 0.02	190.35 ±0.29	0.19 ±0.01	39.50±0.28	28.45±0.07	55.43 ± 0.05	220.10 ±0.71	0.15 ±0.00	30.57±0.17	30.75±0.07	55.67 ± 0.06

Physical and chemical properties of sweetgum bark extract loaded nanoparticles produced by nanoprecipitation, high homogenization speed and ultrasonic homogenization methods.

Table 5
Physical and chemical properties of sweetgum bark extract loaded ZNPs produced by nanoprecipitation, high homogenization speed and ultrasonic homogenization methods.

Exp.	Sweetgum bark extract loaded ZNPs by nanoprecipitation					Sweetgum bark extract loaded ZNPs by high homogenization speed					Sweetgum bark extract loaded ZNPs by ultrasonic homogenization				
	Particle size (nm)	PDI (%)	Transmittance	Zeta potential (mV)	EE (%)	Particle size (nm)	PDI (%)	Transmittance	Zeta potential (mV)	EE (%)	Particle size (nm)	PDI (%)	Transmittance	Zeta potential (mV)	EE (%)
1	132.81 ±0.47	0.15 ±0.00	79.50±0.11	26.97±0.25	95.01 ± 0.04	165.88 ±0.25	0.13 ±0.00	69.92±0.03	27.55±0.49	95.08 ± 0.02	167.60 ±0.48	0.10 ±0.00	64.55±0.07	31.75±0.21	95.18 ± 0.15
2	158.89 ±0.11	0.09 ±0.01	52.45±0.07	28.47±0.35	95.38 ± 0.08	186.48 ±0.32	0.13 ±0.01	32.20±0.00	28.50±0.00	95.57 ± 0.06	196.83 ±0.06	0.10 ±0.00	27.50±0.14	32.17±0.18	95.50 ± 0.08
3	140.73 ±0.27	0.13 ±0.01	77.55±0.35	29.37±0.07	94.97 ± 0.04	161.45 ±0.07	0.12 ±0.01	64.62±0.03	25.33±0.49	95.07 ± 0.01	171.22 ±0.67	0.11 ±0.00	62.32±0.03	32.33±0.03	95.06 ± 0.03
4	165.48 ±0.14	0.06 ±0.01	50.87±0.03	29.30±0.00	95.53 ± 0.01	226.67 ±0.49	0.23 ±0.01	3.22±0.03	31.25±0.35	95.69 ± 0.10	215.13 ±0.28	0.13 ±0.01	18.10±0.14	33.30±0.11	95.62 ± 0.03
5	149.83 ±0.42	0.14 ±0.01	73.30±0.00	26.50±0.42	95.00 ± 0.07	163.09 ±0.01	0.12 ±0.01	60.40±0.28	28.67±0.25	95.04 ± 0.01	182.46 ±0.28	0.11 ±0.01	56.07±0.11	30.73±0.03	95.00 ± 0.06
6	172.91 ±0.62	0.06 ±0.00	48.30±0.00	29.27±0.03	95.58 ± 0.02	184.54 ±0.06	0.10 ±0.01	36.45±0.35	28.40±0.28	95.66 ± 0.03	233.45 ±0.07	0.18 ±0.01	11.97±0.03	34.10±0.00	95.68 ± 0.09
7	152.56 ±0.31	0.14 ±0.00	69.70±0.14	25.30±0.32	95.02 ± 0.05	162.47 ±0.06	0.12 ±0.00	55.65±0.21	26.05±0.07	95.18 ± 0.01	204.90 ±0.71	0.14 ±0.00	41.55±0.21	32.95±0.07	95.04 ± 0.01
8	166.08 ±0.06	0.10 ±0.00	49.50±0.42	26.53±0.39	95.41 ± 0.12	254.43 ±0.14	0.25 ±0.00	1.32±0.03	33.55±0.35	95.46 ± 0.06	325.50 ±0.64	0.23 ±0.00	1.250±0.07	36.73±0.03	95.42 ± 0.06
9	149.66 ±0.25	0.14 ±0.00	73.67±0.03	28.47±0.03	51.16 ± 0.01	171.68 ±0.10	0.10 ±0.00	62.32±0.03	28.70±0.00	51.28 ± 0.02	185.76 ±0.22	0.11 ±0.00	58.17±0.03	33.50±0.14	51.30 ± 0.01
10	174.32 ±0.54	0.09 ±0.00	42.37±0.11	26.85±0.07	51.42 ± 0.12	186.72 ±0.33	0.11 ±0.01	34.17±0.03	27.60±0.42	51.50 ± 0.00	215.27 ±0.28	0.14 ±0.01	17.42±0.03	34.47±0.14	51.58 ± 0.02
11	145.33 ±0.15	0.12 ±0.01	75.03±0.03	32.37±0.07	51.20 ± 0.02	156.74 ±0.04	0.12 ±0.01	65.70±0.00	27.15±0.07	51.20 ± 0.05	170.46 ±0.33	0.10 ±0.00	62.73±0.07	32.20±0.14	51.21 ± 0.01
12	159.36 ±0.10	0.07 ±0.00	53.67±0.03	33.30±0.14	51.40 ± 0.03	233.57 ±0.39	0.24 ±0.01	0.800±0.00	34.20±0.28	51.58 ± 0.12	221.30 ±0.42	0.13 ±0.03	16.35±0.07	33.35±0.35	51.33 ± 0.03
13	156.54 ±0.06	0.09 ±0.00	72.13±0.03	30.67±0.03	51.23 ± 0.08	148.45 ±0.20	0.13 ±0.00	68.60±0.00	31.45±0.49	51.25 ± 0.05	179.36 ±0.49	0.079 ±0.00	57.05±0.07	31.43±0.18	51.24 ± 0.02
14	177.61 ±0.06	0.04 ±0.02	44.47±0.03	32.33±0.07	51.56 ± 0.08	176.86 ±0.04	0.12 ±0.00	35.35±0.21	30.13±0.39	51.35 ± 0.05	240.25 ±0.78	0.18 ±0.00	11.57±0.03	34.27±0.03	51.42 ± 0.02
15	153.89 ±0.18	0.09 ±0.01	71.60±0.00	34.43±0.03	51.24 ± 0.01	170.35 ±0.52	0.12 ±0.01	61.55±0.14	29.67±0.18	51.22 ± 0.07	191.39 ±0.40	0.11 ±0.00	49.85±0.00	33.15±0.21	51.24 ± 0.06
16	169.21 ±0.07	0.07 ±0.00	44.05±0.07	35.10±0.11	51.43 ± 0.15	273.32 ±0.03	0.25 ±0.00	0.60±0.00	37.45±0.49	51.49 ± 0.01	284.43 ±0.18	0.22 ±0.00	4.80±0.00	34.57±0.14	51.41 ± 0.03
17	152.51 ±0.13	0.15 ±0.01	79.10±0.00	32.87±0.18	66.46 ± 0.01	139.56 ±0.00	0.11 ±0.00	79.25±0.21	32.20±0.14	66.42 ± 0.02	162.43 ±0.51	0.08 ±0.00	76.80±0.00	32.60±0.11	66.44 ± 0.03
18	178.86 ±0.46	0.07 ±0.00	38.55±0.28	34.10±0.00	67.00 ± 0.19	236.10 ±0.42	0.18 ±0.00	3.02±0.03	35.33±0.03	67.01 ± 0.08	268.50 ±0.14	0.19 ±0.01	5.30±0.00	34.00±0.00	67.13 ± 0.15
19	155.87 ±0.04	0.08 ±0.00	60.30±0.21	29.35±0.21	66.69 ± 0.01	162.15 ±0.36	0.09 ±0.01	53.02±0.03	29.65±0.64	66.66 ± 0.02	191.05 ±0.07	0.12 ±0.01	38.77±0.03	33.10±0.00	66.74 ± 0.02
20	155.51 ±0.02	0.06 ±0.01	60.12±0.03	34.13±0.14	66.65 ± 0.03	210.60 ±0.14	0.18 ±0.00	15.74±0.02	32.45±0.07	66.72 ± 0.05	236.20 ±0.00	0.17 ±0.00	26.70±0.00	33.87±0.03	66.76 ± 0.04
21	153.12 ±0.63	0.11 ±0.01	61.27±0.18	30.05±0.21	66.59 ± 0.12	176.41 ±0.44	0.15 ±0.00	46.37±0.14	28.30±0.21	66.77 ± 0.00	189.80 ±0.66	0.12 ±0.00	36.20±0.11	31.50±0.28	66.81 ± 0.05
22	162.40 ±0.11	0.07 ±0.00	58.47±0.03	31.40±0.00	66.68 ± 0.13	208.90 ±0.32	0.18 ±0.03	23.40±0.28	32.00±0.00	66.77 ± 0.02	250.95 ±0.00	0.20 ±0.01	18.80±0.00	32.60±0.00	66.82 ± 0.05
23	153.08 ±0.52	0.11 ±0.00	61.10±0.14	29.85±0.07	–	220.40 ±0.42	0.22 ±0.00	24.35±0.35	29.60±0.57	–	229.60 ±0.42	0.16 ±0.00	24.55±0.00	34.10±0.14	–
24	152.17 ±0.31	0.10 ±0.01	62.15±0.21	33.47±0.07	41.69 ± 0.05	214.17 ±0.57	0.206 ±0.00	19.55±0.14	33.37±0.07	41.75 ± 0.02	225.53 ±0.46	0.14 ±0.00	17.25±0.00	32.25±0.07	41.76 ± 0.01
25	164.34 ±0.03	0.05 ±0.00	62.80±0.14	34.40±0.28	66.72 ± 0.15	214.75 ±0.21	0.18 ±0.00	16.52±0.03	32.33±0.07	66.77 ± 0.03	226.57 ±0.32	0.18 ±0.01	14.37±0.03	33.25±0.07	66.86 ± 0.04
26	156.52 ±0.07	0.06 ±0.00	60.40±0.00	31.30±0.14	66.72 ± 0.04	203.72 ±0.34	0.19 ±0.00	22.35±0.07	33.53±0.07	66.66 ± 0.08	235.27 ±0.67	0.17 ±0.00	15.35±0.07	34.63±0.07	66.81 ± 0.04
27	169.48 ±0.68	0.05 ±0.00	53.50±0.14	30.10±0.14	66.78 ± 0.16	224.57 ±0.60	0.23 ±0.00	10.22±0.03	33.70±0.11	66.77 ± 0.02	227.60 ±0.32	0.17 ±0.06	15.97±0.03	31.87±0.03	66.72 ± 0.07
28	156.56 ±0.35	0.06 ±0.00	60.05±0.00	31.45±0.35	66.73 ± 0.01	231.53 ±0.25	0.19 ±0.01	7.37±0.11	30.30±0.28	66.67 ± 0.02	233.40 ±0.00	0.14 ±0.06	13.32±0.03	33.10±0.14	66.73 ± 0.01
29	153.36 ±0.28	0.07 ±0.01	61.70±0.00	31.25±0.35	66.75 ± 0.07	230.15 ±0.35	0.22 ±0.00	8.67±0.03	35.67±0.03	66.68 ± 0.01	237.37 ±0.28	0.16 ±0.04	13.12±0.03	33.25±0.07	66.80 ± 0.05
30	155.36 ±0.04	0.08 ±0.01	60.05±0.07	32.4 ± 0.42	66.60 ± 0.01	227.20 ±0.14	0.19 ±0.03	9.22±0.03	32.15±0.07	66.70 ± 0.03	238.20 ±0.42	0.15 ±0.04	12.52±0.03	33.30±0.00	66.86 ± 0.01

Table 6
ANOVA results for properties of ZNPs produced by nanoprecipitation, high homogenization speed, ultrasonic homogenization methods.

NPs production methods		Chestnut shell extract-loaded ZNPs			Cedar bark extract-loaded ZNPs			Sweetgum bark extract-loaded ZNPs		
		p values								
		Particle size (nm)	PDI (%)	EE (%)	Particle size (nm)	PDI (%)	EE (%)	Particle size (nm)	PDI (%)	EE (%)
Nanoprecipitation	**X_1-Zein concentration**	0.0019	< 0.0001	< 0.0001	< 0.0001	< 0.0001	0.2937	< 0.0001	< 0.0001	0.4486
	X_6_Mixing speed	0.4641	0.0281	0.2542	0.3191	0.008	0.8287	0.4362	0.4585	0.9689
	X_5-Flow rate	0.0610	0.2952	0.7201	0.0341	0.0058	0.9318	0.0031	0.0037	0.9136
	X_4-Extract ratio	0.0139	< 0.0001	< 0.0001	0.0001	0.044	< 0.0001	0.1026	0.0216	< 0.0001
	$X_1 \times_6$	0.6846	0.4669	0.3309	0.9221	0.6583	0.8998	0.2148	0.2970	0.9647
	$X_1 \times_5$	0.0737	0.9040	0.8209	0.0341	0.0394	0.9075	0.4445	0.7185	0.9818
	$X_1 \times_4$	0.0852	0.0033	0.1765	0.0754	0.6691	0.6447	0.5659	0.0913	0.8265
	$X_6 \times_5$	0.0065	0.8122	0.3035	0.9918	0.0075	0.8148	0.6294	0.0071	0.9232
	$X_6 \times_4$	0.1595	0.8229	0.4849	0.1499	0.9281	0.9741	0.0720	0.9447	0.9880
	$X_5 \times_4$	0.3013	0.3436	0.8945	0.3350	0.6106	0.8699	0.4899	0.0056	0.9684
	X_1^2	< 0.0001	< 0.0001	0.0071	0.0041	0.7319	0.2047	0.1356	< 0.0001	0.2316
	X_6^2	0.0256	0.0326	0.8626	< 0.0001	0.0889	0.1909	0.3774	0.1750	0.2593
	X_5^2	0.8383	0.0643	0.9665	0.0465	0.1573	0.2583	0.6984	0.0044	0.2772
	X_4^2	0.0363	0.0081	< 0.0001	0.5309	0.385	< 0.0001	0.1153	0.0001	< 0.0001
	Lack of fit	0.1951	0.6118	< 0.0001	0.1899	0.5815	< 0.0001	0.7930	0.5680	< 0.0001
	R^2	0.9056	0.9482	0.9753	0.9340	0.8370		0.8690	0.9330	
	R^2_{adj}	0.8176	0.8999	0.9523	0.8710	0.6850		0.7480	0.8710	
High speed homogenization	**X_1-Zein concentration**	< 0.0001	< 0.0001	< 0.0001	< 0.0001	< 0.0001	0.1092	< 0.0001	< 0.0001	0.4275
	X_3_Homogenization rate	< 0.0001	0.5110	0.5177	< 0.0001	< 0.0001	0.8163	< 0.0001	< 0.0001	0.9567
	X_2-Time	0.1232	0.9211	0.0618	0.0022	0.0035	0.8023	0.0386	0.266	0.9512
	X_4-Extract ratio	0.8698	< 0.0001	< 0.0001	0.1997	0.6397	< 0.0001	0.9963	0.7787	< 0.0001
	$X_1 \times_3$	0.0018	0.8643	0.8450	< 0.0001	0.0005	0.9236	< 0.0001	< 0.0001	0.9763
	$X_1 \times_2$	0.6138	0.9780	0.8729	0.0211	0.6378	0.8064	0.1089	0.8553	0.9090
	$X_1 \times_4$	0.0002	< 0.0001	0.0017	0.9178	0.2251	0.4555	0.5505	0.6139	0.8029
	$X_3 \times_2$	0.6032	0.3338	0.9761	0.0146	0.6980	0.6072	0.0081	0.4642	0.9882
	$X_3 \times_4$	0.4644	0.0544	0.9701	0.9461	0.3470	0.8849	0.2684	0.5340	0.9893
	$X_2 \times_4$	0.7105	0.0874	0.7502	0.2862	0.8047	0.9482	0.9244	0.3109	0.9664
	X_1^2	< 0.0001	0.0150	0.7495	< 0.0001	0.9056	0.2591	0.0001	0.0006	0.2331
	X_3^2	0.0009	0.1898	0.3987	< 0.0001	0.0193	0.3297	< 0.0001	0.0001	0.2417
	X_2^2	0.0032	0.3920	0.0688	0.5110	0.6500	0.1894	0.0004	0.005	0.2068
	X_4^2	0.0007	0.3037	< 0.0001	0.8790	0.3132	< 0.0001	0.2279	0.8046	< 0.0001
	Lack of fit	0.2046	0.3987	0.0982	0.1098	0.8517	0.0019	0.6695	0.5926	< 0.0001
	R^2	0.9425	0.9181	0.9963	0.9840	0.9150		0.9570	0.9330	
	R^2_{adj}	0.8888	0.8416	0.9925	0.9690	0.8360		0.91700	0.8710	
Ultrasonic homogenization	**X_1-Zein concentration**	< 0.0001	< 0.0001	< 0.0001	< 0.0001	< 0.0001	0.1965	< 0.0001	< 0.0001	0.4184
	X_7-Amplitude	0.1074	0.0899	0.9079	0.0203	0.0015	0.9066	< 0.0001	0.0001	0.9160
	X_2-Time	0.0027	0.9966	0.9089	0.0098	0.5985	0.5953	< 0.0001	< 0.0001	0.9529
	X_4-Extract ratio	0.5949	0.0095	< 0.0001	< 0.0001	0.1400	< 0.0001	0.6903	0.1110	< 0.0001
	$X_1 \times_7$	0.1779	0.6693	0.7671	0.0219	0.8639	0.9642	0.0011	0.1085	0.9524
	$X_1 \times_2$	0.4294	0.1274	0.6089	0.1762	0.0191	0.9399	0.0001	< 0.0001	0.9749
	$X_1 \times_4$	0.0008	< 0.0001	0.0122	0.0251	0.4559	0.8183	0.7636	0.0664	0.7697
	$X_7 \times_2$	0.3402	0.8528	0.5781	0.0157	0.0006	0.9525	0.0003	0.0115	0.9804
	$X_7 \times_4$	0.4926	0.4713	0.7501	0.0081	0.7753	0.7627	0.0194	0.2224	0.9730
	$X_2 \times_4$	0.0519	0.1385	0.6743	0.0268	0.0783	0.6751	0.0159	0.0326	0.9773
	X_1^2	0.7958	0.0025	0.4742	0.1626	0.3702	0.4365	0.0033	0.0011	0.2399
	X_7^2	0.0732	0.6284	0.1274	0.091	0.0049	0.4425	0.0019	0.0114	0.2575
	X_2^2	0.3915	0.4212	0.2634	0.7559	0.0062	0.9558	0.0155	0.4010	0.2268
	X_4^2	0.9189	0.789	< 0.0001	0.6523	0.0804	< 0.0001	0.1245	0.1099	< 0.0001
	Lack of fit	0.2090	0.6693	0.0024	0.0520	0.3756	0.0028	0.0698	0.7786	< 0.0001
	R^2	0.8967	0.8973	0.9916	0.9520	0.8860		0.9720	0.9570	
	R^2_{adj}	0.8003	0.8015	0.9831	0.9070	0.7800		0.9460	0.9170	

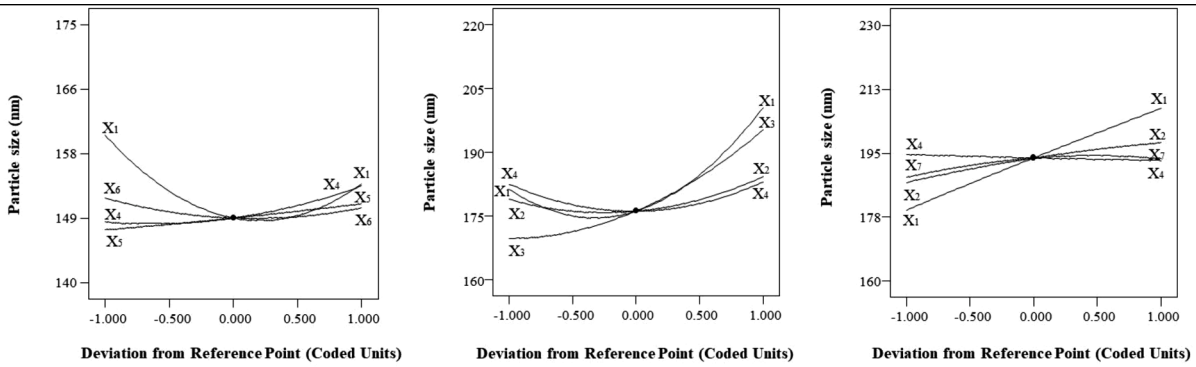

1.a. Perturbation graphs for particle size of chestnut shell extract loaded nanoparticles produced by nanoprecipitation, high homogenization speed and ultrasonic homogenization methods

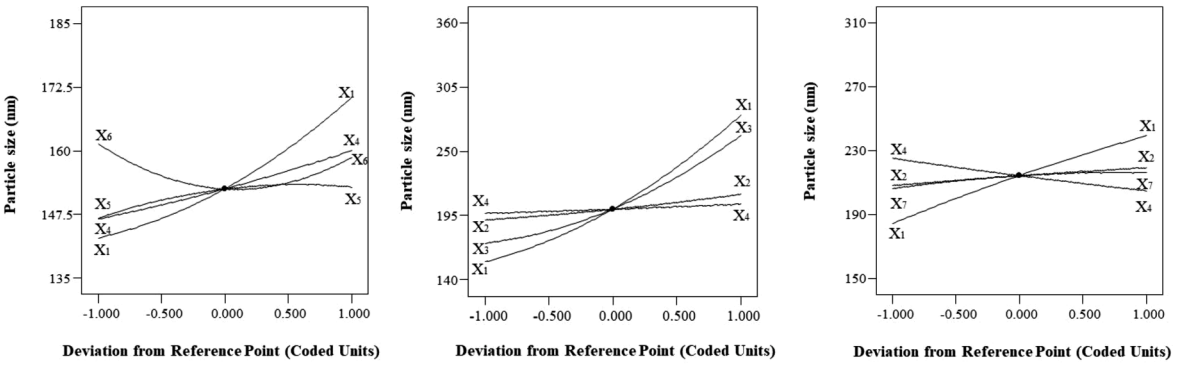

1.b. Perturbation graphs for particle size of cedar bark extract loaded nanoparticles produced by nanoprecipitation, high homogenization speed and ultrasonic homogenization methods

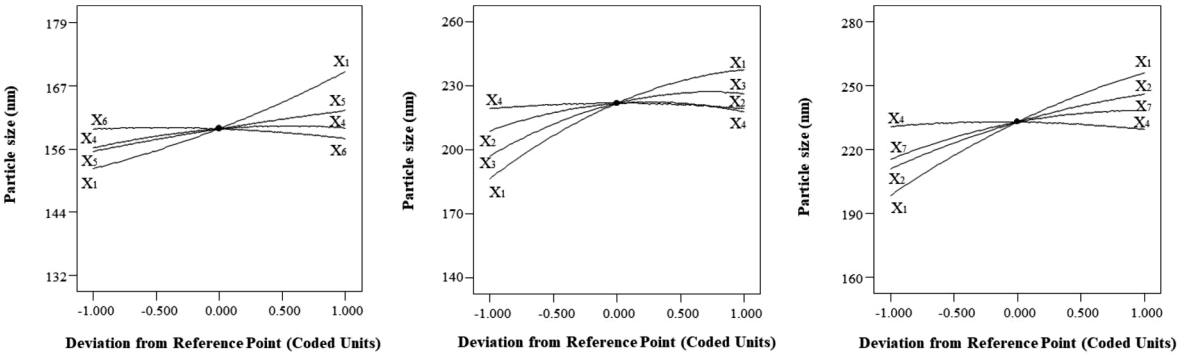

1.c. Perturbation graphs for particle size of sweetgum bark extract loaded nanoparticles produced by nanoprecipitation, high homogenization speed and ultrasonic homogenization methods

Fig. 1. Perturbation graphs belongs to particle size of extract loaded nanoparticles produced by nanoprecipitation, high homogenization speed and ultrasonic homogenization methods.

2017). These findings point to a range of zein-caseinate ratios to produce nanoparticles with small particle sizes.

The diameters of ZNPs loaded with chestnut, cedar and sweetgum shell/bark extracts by high-speed homogenization method were in the range of 169.37 and 254.75 nm (Table 3), 155.61 and 430.25 nm (Table 4), and 139.56 and 273.33 nm (Table 5), respectively. For all three extract types, the most important factors influencing the size of nanoparticles are zein concentration, homogenization rate and the interaction of zein concentration and homogenization rate. The perturbation graph revealed the effect of zein concentration and homogenization rate on the particle size (Fig. 1). As with the nanoprecipitation method for chestnut shell extract, a saddle system was found due to the zein concentration and homogenization rate interaction, as seen in Fig. 1a. From Fig. 1b and c, it is clear that an increase in homogenization rate and zein concentration led to an increase in particle diameter of cedar and sweetgum bark extract-loaded NPs. As the zein concentration increases, the consistency index of the solution increases. This situation increases the resistance to the processes (mixing, homogenization speed, amplitude) applied during nanoparticle production, especially at high zein concentrations. The particle size increases as the resistance increases and the applied processes' effectiveness decreases. Excessive energy input at high homogenization rates increases the impact frequency between the particles in the system, leading to coalescence and the formation of larger particles. In addition,

a high homogenization rate causes protein denaturation, leading to aggregation.

The hydrodynamic diameters of nanoparticles containing chestnut, cedar and sweetgum shell/bark extracts obtained by using the ultrasonic homogenization method, which is the third nanoparticle production method, ranged from 156.57 to 232.45 nm (Table 3), 153.61 to 300.60 nm (Table 4), and 162.45 to 325.50 nm (Table 5), respectively. Zein concentration and sonication time affect particle size in chestnut extract-based nanoparticles. The particle diameter increased as the zein concentration and sonication time increased. On the other hand, the particle diameter of nanoparticles loaded with cedar bark extract is affected by all process variables. An increase was observed in particle diameter with increasing zein concentration, amplitude value and sonication time, while a decrease was observed in particle diameter with increasing extract ratio.

Similarly, in nanoparticles containing sweetgum bark extract, the particle diameter increased as the zein concentration, amplitude value, and sonication time increased. As the sonication time increases, smaller particles are formed, and therefore the surface area of the nanoparticles increases. Increasing the surface area gives the nanoparticles very high surface energy. In addition, the increase in temperature with the sonication process also increases the kinetic energies of the particles. Nanoparticles form agglomeration to minimize this surface energy. In addition, uncontrolled agglomeration may occur in nanoparticles due to attractive van der Waals forces between particles. Another factor that increases the particle size is nanoparticle aggregation due to the formation of covalent bonds. In addition, the increase in temperature and mixing speed with the increase in amplitude and time can cause protein denaturation and, thus, aggregation.

The particle sizes of nanoparticles produced using different methods—namely, nanoprecipitation, high-speed homogenization, and ultrasonic homogenization—under various process conditions exhibited variations. For chestnut shell extract, the sizes ranged between 143.47–187.23 nm, 169.37–254.75 nm, and 156.57–232.45 nm for the respective methods. Similarly, for cedar bark extract, sizes were 136.27–202.40 nm, 155.61–430.25 nm, and 153.61–300.60 nm, while for sweetgum bark extract, they ranged from 132.81 to 178.87 nm, 139.56–273.33 nm, and 162.45–325.50 nm. Despite using the same coating materials, each method has its advantages and limitations. Notably, nanoprecipitation excels in achieving smaller particle sizes and maintaining bioactivity due to the absence of heat generation. On the other hand, high-speed homogenization and ultrasonic homogenization involve heat generation, potentially increasing particle kinetic energy, leading to particle aggregation and reduced energy. This difference likely contributes to the smaller dimensions of nanoparticles obtained via nanoprecipitation compared to the other methods. Yang et al. (2023) have mentioned a similar phenomenon. The antisolvent precipitation method successfully formed pure zein nanoparticles with a mean particle size of 124.5 nm and quercetin-resveratrol-loaded zein nanoparticles had larger particle sizes, changing approximately between 200 and 400 nm. Studies in the literature presented higher particle size values as 195.4 nm for zein nanoparticles loaded with curcumin Liu et al. (2019), 253 nm for zein nanoparticles loaded with rutin Zhang and Han (2018), 204.8 nm for zein nanoparticles loaded with thymol (Zhang et al., 2014) by using 1:1 ratio of zein: sodium caseinate. The presented study has shown that zein can produce bioactive extract-loaded nanoparticles with small particle sizes (minimum 132.81 nm), which indicates good performance. We assessed the stability of optimized zein nanoparticles, containing chestnut shell extract. Those were stored at 4 °C and 25 °C for 90 days. We tracked changes in particle size, polydispersity index, transmittance, zeta potential, and encapsulation efficiency (unpublished data). Results emphasized temperature's impact on their physical attributes. Superior stability was seen at 4 °C compared to 25 °C. Encapsulation efficiency declined over time, especially at 25 °C. Particle size at 25 °C showed significant fluctuations (138.82 to 232.62 nm), while at 4 °C, it remained steadier (138.82 to 155.88 nm). It can be concluded that the temperature plays a key role in enhancing stability of zein nanoparticles.

Polydispersity index (PDI)

The polydispersity index is crucial in estimating the average homogeneity of the suspension/emulsion. The numerical value of the PDI ranges from 0.0 to 1.0. When this value approaches 1, it represents a multi-distribution system; when it approaches zero, it represents a mono-distribution system. Polydisperse systems tend to aggregate more than monodisperse systems. For PDI, values of 0.2 and below in polymer-based nanoparticles (Clarke, 2013) and values of 0.3 and below in drug release applications using lipid-based carriers as liposome and nanoliposomes formulations are considered appropriate (Badran, 2014; Chen, Liu & Fahr, 2011; Putri, Dwiastuti & Marchaban, 2017).

PDI of chestnut shell extract-loaded ZNPs produced by nanoprecipitation, high-speed homogenization, and ultrasonic homogenization methods varied in the range of 0.078 and 0.265%, 0.064 and 0.262%, and 0.078 and 0.234%, respectively, and the change intervals were generally close to each other. The most important process variables affecting the PDI for all three methods were zein concentration and extract ratio. The results were shown that whereas the higher zein concentration resulted in a smaller PDI, a higher extract ratio ended up with a larger PDI (Fig. 2a).

PDI of nanoparticles containing cedar bark extract varied between 0.03 and 0.15%, 0.10 and 0.27%, and 0.08 and 0.20% for nanoprecipitation, homogenization and ultrasonic methods, respectively. The minimum polydispersity values were obtained in nanoparticles produced by the nanoprecipitation method. PDI of ZNPs loaded with cedar extract by nanoprecipitation method is affected statistically ($p < 0.05$) by all process variables (Table 6), including zein concentration, mixing speed, flow rate and extract amount. The findings revealed that the PDI increased with decreasing zein concentration and extract ratio and increasing flow rate and mixing speed. The PDI of ZNPs loaded with cedar bark extract obtained by the high-speed homogenization method is significantly affected by zein concentration, homogenization speed and time. As seen in Fig. 2b, the PDI was maximum when these variables were maximized. PDI of ZNPs, including cedar bark extract, is affected by zein concentration and amplitude variables at a statistically significant ($p < 0.05$) level in the ultrasonic homogenization method (Table 6). An increase in PDI of nanoparticles was caused by an increase in amplitude value, as well as an increase in zein concentration. Depending on the method used in nanoparticles containing cedar extract, the interaction of zein concentration with applied mixing speed, homogenization speed and amplitude value was also found to be effective on PDI.

PDI of nanoparticles, including sweetgum bark extract produced by the nanoprecipitation method, varied between 0.044 and 0.153%. In this method, PDI is affected by the flow rate, the extract ratio and especially the zein concentration. The minimum value was observed under the conditions where these process variables are maximum. In the high-speed homogenization method, the PDI of nanoparticles varies between 0.087 and 0.254%, and it is affected by the zein concentration, homogenization rate and the interaction of these two process variables. As the zein concentration and homogenization rate increased, the PDI value increased. PDI values of nanoparticles obtained by the ultrasonic homogenization method are in the range of 0.080 and 0.234% and are statistically affected by zein concentration, amplitude value and sonication time. When these process variables are maximum, the PDI value is also maximum. The perturbation graph (Fig. 2c) illustrates the changes in PDI related to the process factors of each method for nanoparticles, including sweetgum bark extract.

Regarding the polydispersity of ZNPs, the variation intervals for high-speed homogenization and ultrasonic homogenization methods were close and higher than the nanoprecipitation method. It indicates that the extract-loaded ZNPs produced by the nanoprecipitation method

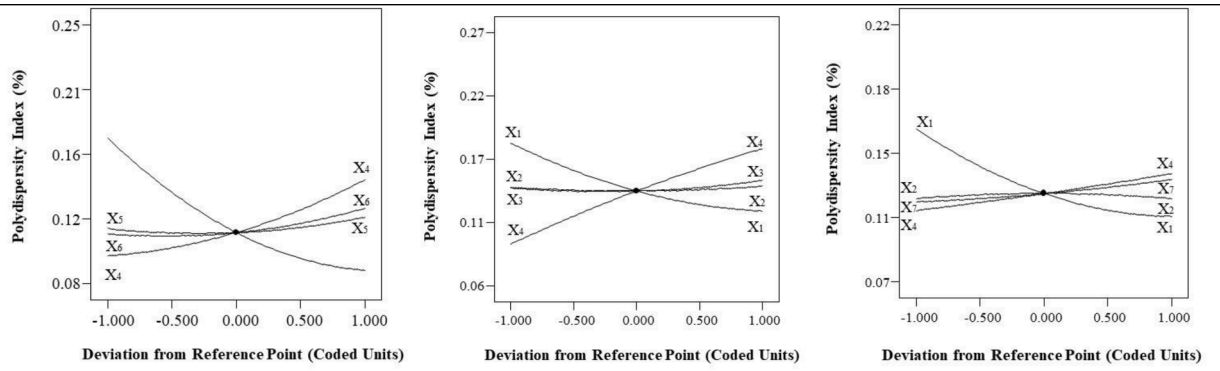

2.a. Perturbation graphs for polydispersity index of chestnut shell extract loaded nanoparticles produced by nanoprecipitation, high homogenization speed and ultrasonic homogenization methods

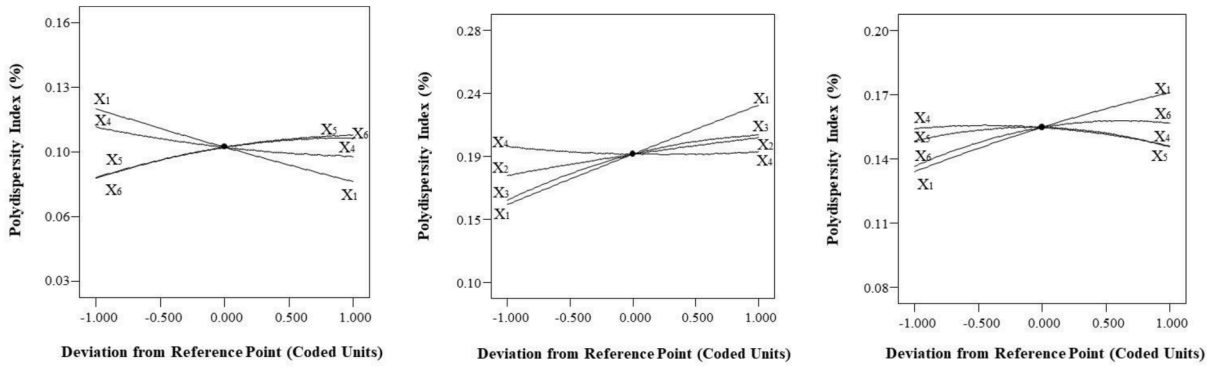

2.b. Perturbation graphs for polydispersity index of cedar bark extract loaded nanoparticles produced by nanoprecipitation, high homogenization speed and ultrasonic homogenization methods

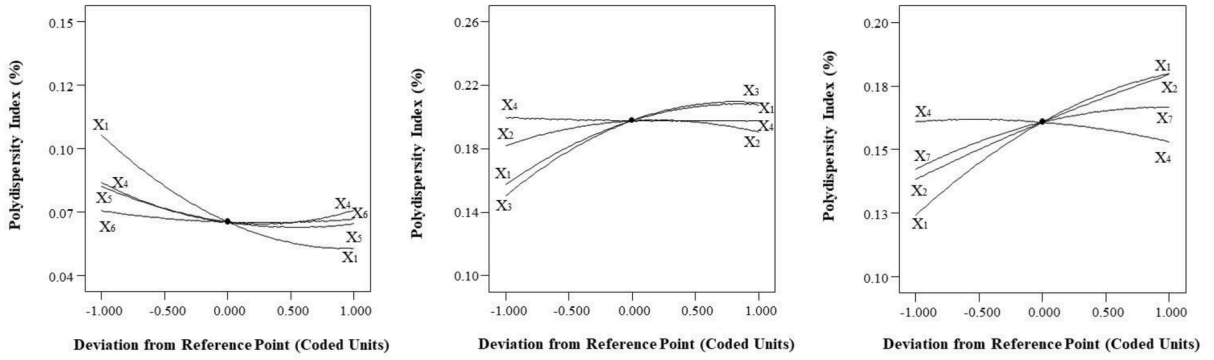

2.c. Perturbation graphs for polydispersity index of sweetgum bark extract loaded nanoparticles produced by nanoprecipitation, high homogenization speed and ultrasonic homogenization methods

Fig. 2. Perturbation graphs belongs to polydispersity index of extract loaded nanoparticles produced by nanoprecipitation, high homogenization speed and ultrasonic homogenization methods.

have a more homogeneous structure and a narrower size distribution. The zein concentration was the most critical process variable affecting the PDI for all three methods (Fig. 2). In the high-speed homogenization and ultrasonic homogenization methods, the PDI values increased with the increase of the zein concentration. In contrast, the opposite was observed in the nanoprecipitation method, and the increase in the zein concentration decreased the PDI value.

Zeta potential

The zeta potential is used to measure the surface charge of nanoparticles in the colloidal system and directly influences nanosuspensions' stability (Jiang, Oberdörster & Biswas, 2009). The Zeta potential of nanoparticles with values $>+25$ mV or <-25 mV is usually considered to have high physical stability. Nanodispersions with high zeta potential (positive or negative) are electrically stabilized, indicating a highly stable system. In contrast, dispersions with low zeta potentials are prone to aggregate, flocculate or coagulate, owing to van der Waals interparticle attraction, resulting in a relatively unstable system (Horie & Fujita, 2011; Sapsford, Tyner, Dair, Deschamps & Medintz, 2011).

The zeta potentials of caseinate-stabilized ZNPs obtained by nanoprecipitation, high-speed homogenization and ultrasonic

homogenization methods ranged between (−34.00) and (−42.75)mV, (−29.40) and (−42.30)mV and (−33.25) and (−40.98)mV, respectively in chestnut extract-loaded ZNPs, (−31.35) and (−33.70)mV, (−28.45) and (−39.40)mV and (−23.25) and (−32.73)mV, respectively in cedar extract loaded ZNPs and (−25.30) and (−35.10)mV, (−25.33) and (−37.45)mV and (−30.73) and (−36.73)mV, respectively in sweetgum extract loaded ZNPs. Generally, zeta potentials for all three methods are more than −30 mV for chestnut extract-loaded ZNPs and −25 mV for cedar and sweetgum extracts loaded caseinate stabilized ZNPs. The zeta potential of the obtained nanoparticles has a narrow range of variation and is mostly higher than −25 mV, which indicates high physical stability in suspension.

Transmittance

The high transmittance value is accepted as a good indicator of the nano-sized scale of the zein particle suspension (Boufi et al., 2018). In the nanoprecipitation method, the smaller size and higher transmittance values of the nanoparticles confirm this situation. However, zein concentration and extract ratio, typical process variables for all three methods, affect the transmittance. The transmittance of the suspension changed during mixing, homogenization and sonication. The effect of zein concentration was seen mainly in zein nanoparticle suspensions that did not contain extracts and were prepared at different concentrations. The increase in the zein concentration showed a significant decrease in the transmittance value. In addition, the extract ratio affects the color of the suspension as well as the transmittance value.

The transmittance values of nanoparticles produced by nanoprecipitation, high homogenization speed and ultrasonic homogenization varied between 34.40 and 73.48, 15.38 and 71.85, and 10.53 and 53.88, respectively, for chestnut shell extract containing NPs; 29.40 and 79.10, 0.20 and 77.45, and 2.80 and 80.18, respectively for cedar bark extract containing NPs and 38.55 and 79.50, 0.60 and 79.25, and 1.25 and 76.80, respectively for sweetgum bark extract containing NPs. When the effects of different process variables and nanoparticle production methods on the transmittance values of nanoparticles are evaluated on a method basis, the order of transmittance from high to low is nanoprecipitation, ultrasonic homogenization, and high-speed homogenization, respectively. It was observed that the nanoparticle suspensions obtained by the nanoprecipitation method were generally more transparent compared to the ultrasonic and high-speed homogenization methods during the experiments. Especially in the high-speed homogenization method, the suspensions became translucent with increased homogenization rate and zein concentration.

Encapsulation efficiency

The effects of the nanoparticle production methods and process conditions on the EE of ZNPs were investigated. At the stage of determining the appropriate model for the EE of ZNPs produced by nanoprecipitation, high-speed homogenization and ultrasonic extraction methods, in the 23rd trial, which included the condition that the extract ratio was minimum, EE was calculated above 100% for nanoprecipitation, high-speed homogenization and ultrasonic extraction methods. Since this situation is due to the limited extract ratio, which could not be detected and caused the experimental error, EE could not be measured for all three trial methods. For this reason, the 23rd trial was not included in the model for all three methods of modeling the EE.

EE in ZNPs encapsulated with chestnut shell extract was found to vary between 38.90 and 96.83%, 39.46 and 96.11%, and 39.18 and 95.00% for nanoprecipitation, high-speed homogenization and ultrasonic homogenization methods, respectively. EE values were quite close to each other for the homogenization and nanoprecipitation methods and higher when compared to the ultrasonic method. The zein concentration and especially the extract ratio significantly affected the EE of nanoparticles. As the extract ratio increased, a significant decrease was observed in the EE of the nanoparticles. Other researchers have encountered a similar situation in encapsulation studies with retinol (Park, Park & Kim, 2015), α tocopherol (Luo, Zhang, Whent, Yu & Wang, 2011), vitamin E (Liu & Park, 2009), and curcumin Liu et al. (2019). The EE increased with the increase of zein concentration. Liang et al. (2017) reported that EE increased from 65.0% to 80.7% with the increment of zein concentration from 72 to 288 mg. The EE of nanoparticles containing cedar bark extract was between 34.61 and 79.17%, 35.10 and 79.66%, and 34.03 and 78.84% for nanoprecipitation, high-speed homogenization and ultrasonic homogenization methods, respectively. The EE of the sweetgum bark extract nanoparticles varied in the ranges of 41.69% and 95.58%, 41.75% and 95.69% and 41.76% and 95.68% for nanoprecipitation, high-speed homogenization and ultrasonic homogenization methods, respectively. The EE of nanoparticles loaded with cedar and sweetgum bark extracts was significantly affected only by the extract ratio. As the extract ratio increased, a significant decrease was observed in the EE of the nanoparticles. Curcumin-fortified ZNPs with high EE in the range of 86.8 and 91.8% were reported by Hu et al. (2015), and similarly, curcumin loading efficiency decreased as the curcumin content increased. Correlatively, the ANOVA results (Table 6) indicated that the common process variable which significantly ($p < 0.05$) affected encapsulation efficiency of nanoparticle was the extract ratio in all methods. As the amount of dissolved extract increase, the encapsulation efficiency decreased. The reason for this may be that some extract is carried within the caseinate structure without being able to hold on to the zein structure.

When the effect of the nanoparticle production method on the EE was examined, it was observed that the encapsulation efficiencies were very close to each other for all three methods. However, the EE was the lowest in nanoparticles containing cedar extract, possibly related to the extract properties. In the literature, many studies based on zein nanoparticles were performed to encapsulate and protect bioactive compounds, essential oils or functional ingredients. EE of zein nanoparticles differentiates according to the encapsulated component and production method. Recently, Liu et al. (2022) developed curcumin-loaded zein-tea saponin nanoparticles with 80% and 71% EE using antisolvent co-precipitation and precipitation methods, respectively. Furthermore, zein and polysaccharide-based nanoparticles are an alternative to carry antioxidant compounds such as quercetin, anthocyanin, resveratrol, epigallocatechin gallate and others by providing excellent stability (Tapia-Hernández et al., 2018). Yang et al. (2023) reported that the encapsulation of quercetin and resveratrol in zein- carboxymethyl cellulose nanoparticles had EE values of 43.5% and 25.1%, respectively. The EE of quercetin were higher in zein-carboxymethyl cellulose nanoparticles than in resveratrol. It is important to study the different concentrations of zein and different amount of encapsulated compound in nanoparticles to obtain high EE. Besides, nanoparticle fabrication methods can contribute to the EE of nanoparticles. In this study, the EE of ZNPs had considerably higher values compared to studies in the literature.

TEM analysis

The arrangement of nanoparticles within the film structure was examined using TEM images, displayed in Fig. 3, showcasing active nanocomposite films containing zein nanoparticles loaded with diverse extract types. These zein nanoparticle-loaded extracts appear as dark formations, while the biopolymer matrix is transparent. Although the film structure predominantly showed even distribution, certain areas exhibited asymmetrical molecules. Zein nanoparticles are randomly dispersed within the composite film matrix, with integrated or uneven distribution suggesting interaction between nanoparticles and the polymer matrix. Notably, a significant difference emerged in active nanocomposite films incorporating nanoparticles with sweetgum bark extract, as depicted in Fig. 3c, showing instances of agglomeration. Despite all nanoparticles encapsulating chestnut shell, cedar, and

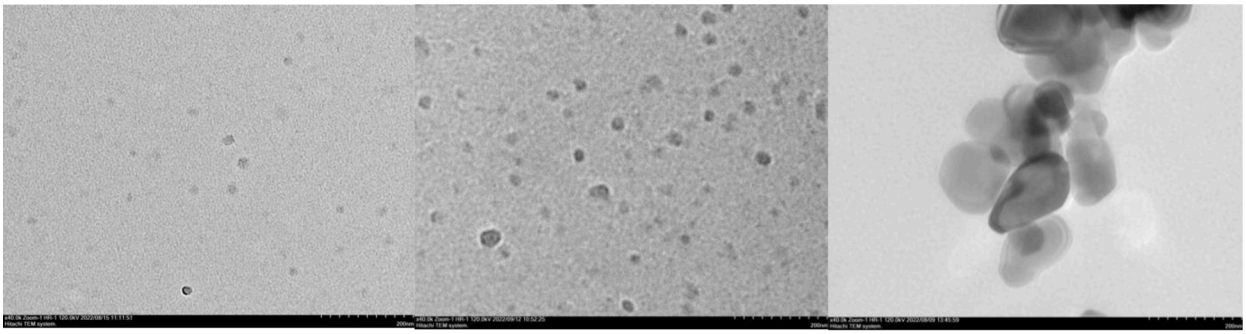

Fig. 3. TEM images of zein nanoparticles in the structure of active nanocomposite films incorporated with nanoparticles containing chestnut shell extract (a), cedar bark extract (b) and sweetgum bark extract (c).

sweetgum bark extracts being produced under optimal conditions, the composition variations, particularly the higher oil content in sweetgum bark extract, could lead to droplet coalescence. Additionally, insufficient protein content might fail to envelop lipid molecules within the extract.

Conclusion

Caseinate-stabilized ZNPs were developed to encapsulate chestnut, cedar and sweetgum shell/bark extracts from natural sources rich in bioactive substances. Effects of process conditions on the physical and chemical properties of chestnut, cedar and sweetgum waste extract-loaded ZNPs were investigated with three different methods: nano-precipitation, high-speed homogenization, and ultrasonic homogenization. Zein concentration was found as the most effective process variable on the physical properties of nanoparticles. The extract ratio significantly influences the EE of ZNPs. It was observed that the nano-precipitation method is more suitable for providing minimum particle size, minimum PDI and maximum EE in chestnut and cedar waste extract-loaded ZNPs. The high-speed homogenization method with small particle sizes is more suitable for producing nanoparticles loaded with sweetgum bark extract. ZNPs fabricated at selected conditions are promising for carrying bioactive extracts into food products, nutraceuticals or active food packaging systems. Further studies on active food packaging are going on by the same research team.

Ethical statement

The research presented does not involve any animal or human study.

CRediT authorship contribution statement

Dilara Konuk Takma: Investigation, Methodology, Formal analysis, Data curation, Writing – original draft. **Semra Bozkurt:** Methodology, Formal analysis, Data curation, Writing – original draft. **Mehmet Koç:** Conceptualization, Methodology, Writing – review & editing. **Figen Korel:** Conceptualization, Methodology, Writing – review & editing. **Hilal Şahin Nadeem:** Conceptualization, Methodology, Supervision, Project administration, Writing – review & editing.

Declaration of Competing Interest

The authors declare that they have no known competing financial interests or personal relationships that could have appeared to influence the work reported in this paper.

Data availability

No data was used for the research described in the article.

Acknowledgements

The authors acknowledge TUBITAK-TOVAG (Project Number: 119O334) for financial support and Dr. Said Nadeem for proofreading.

References

Ahmed, O. A., Hosny, K. M., Al-Sawahli, M. M., & Fahmy, U. A. (2015). Optimization of caseinate-coated simvastatin-zein nanoparticles: Improved bioavailability and modified release characteristics. *Drug Design, Development and Therapy, 9*, 655.

Anton, N., Benoit, J.-P., & Saulnier, P. (2008). Design and production of nanoparticles formulated from nano-emulsion templates—A review. *Journal of controlled release, 128*(3), 185–199.

Badran, M. (2014). Formulation and in vitro evaluation of flufenamic acid loaded deformable liposomes for improved skin delivery. *Digest Journal of Nanomaterials & Biostructures (DJNB), 9*(1).

Bal Öztürk, A. (2015). *Hedeflendirilmiş polimerik nanopartiküler taşıyıcı sistemlerin geliştirilmesi*. İstanbul: İstanbul Üniversitesi Fen Bilimleri Enstitüsü (Doktora Tezi).

Boufi, S., Haaj, S. B., Magnin, A., Pignon, F., Impéror-Clerc, M., & Mortha, G. (2018). Ultrasonic assisted production of starch nanoparticles: Structural characterization and mechanism of disintegration. *Ultrasonics Sonochemistry, 41*, 327–336.

Chen, M., Liu, X., & Fahr, A. (2011). Skin penetration and deposition of carboxyfluorescein and temoporfin from different lipid vesicular systems: In vitro study with finite and infinite dosage application. *International Journal of Pharmaceutics, 408*(1-2), 223–234.

Chutia, H., & Mahanta, C. L. (2021). Properties of starch nanoparticle obtained by ultrasonication and high pressure homogenization for developing carotenoids-enriched powder and Pickering nanoemulsion. *Innovative Food Science & Emerging Technologies, 74*, Article 102822.

Clarke, S. (2013). *Development of hierarchical magnetic nanocomposite materials for biomedical applications*. Dublin City University.

Derwich, E., Benziane, Z., & Boukir, A. (2010). Chemical composition and in vitro antibacterial activity of the essential oil of Cedrus atlantica. *International Journal of Agriculture and Biology, 12*(3), 381–385.

Ebert, S., Koo, C. K., Weiss, J., & McClements, D. J. (2017). Continuous production of core-shell protein nanoparticles by antisolvent precipitation using dual-channel microfluidization: Caseinate-coated zein nanoparticles. *Food Research International, 92*, 48–55.

Erdoğdu, Ö. (2021). *Determination of optimum extraction conditions for Toros cedar, styrax tree and chestnut shells and investigation of bioactive properties of extract*. Turkey: Graduate School of Natural and Applied Sciences, Aydın Adnan Menderes University. MSc Thesis.

Gahruie, H. H., Ziaee, E., Eskandari, M. H., & Hosseini, S. M. H. (2017). Characterization of basil seed gum-based edible films incorporated with Zataria multiflora essential oil nanoemulsion. *Carbohydrate Polymers, 166*, 93–103.

Gönültaş, O., & Sarıalan, N. (2017). Toros Sediri (Cedrus libani) kabuk taneninin fenolik bileşimi. *Kastamonu Üniversitesi Orman FakültesiDergisi*.

Gullón, B., Eibes, G., Dávila, I., Moreira, M. T., Labidi, J., & Gullón, P. (2018). Hydrothermal treatment of chestnut shells (Castanea sativa) to produce oligosaccharides and antioxidant compounds. *Carbohydrate Polymers, 192*, 75–83.

Guzey, D., & McClements, D. J. (2006). Formation, stability and properties of multilayer emulsions for application in the food industry. *Advances in Colloid and Interface Science, 128*, 227–248.

Horie, M., & Fujita, K. (2011). *Toxicity of metal oxides nanoparticles Advances in molecular toxicology, 5* pp. 145–178). Elsevier.

Hu, K., Huang, X., Gao, Y., Huang, X., Xiao, H., & McClements, D. J. (2015). Core–shell biopolymer nanoparticle delivery systems: Synthesis and characterization of curcumin fortified zein–pectin nanoparticles. *Food Chemistry, 182*, 275–281.

Jiang, J., Oberdörster, G., & Biswas, P. (2009). Characterization of size, surface charge, and agglomeration state of nanoparticle dispersions for toxicological studies. *Journal of Nanoparticle Research, 11*(1), 77–89.

Joye, I. J., & McClements, D. J. (2013). Production of nanoparticles by anti-solvent precipitation for use in food systems. *Trends in Food Science & Technology, 34*(2), 109–123.
Kasımoğlu, Z., Yıldırım, A., Alkan, S., Topuz, A., & Nadeem, H.Ş. (2016). Microencapsulation of chestnut seedcoat's water extract by spray drying. *Journal of Ongoing Chemical Research, 2*(2), 34–44.
Lammari, N., Louaer, O., Meniai, A. H., & Elaissari, A. (2020). Encapsulation of essential oils via nanoprecipitation process: Overview, progress, challenges and prospects. *Pharmaceutics, 12*(5), 431.
Li, H., Xu, Y., Sun, X., Wang, S., Wang, J., Zhu, J., Wang, D., & Zhao, L. (2018). Stability, bioactivity, and bioaccessibility of fucoxanthin in zein-caseinate composite nanoparticles fabricated at neutral pH by antisolvent precipitation. *Food Hydrocolloids, 84*, 379–388.
Liang, J., Yan, H., Wang, X., Zhou, Y., Gao, X., Puligundla, P., & Wan, X. (2017). Encapsulation of epigallocatechin gallate in zein/chitosan nanoparticles for controlled applications in food systems. *Food Chemistry, 231*, 19–24.
Liu, C., Xu, B., McClements, D. J., Xu, X., Cui, S., Gao, L., Zhou, L., Xiong, L., Sun, Q., & Dai, L. (2022). Properties of curcumin-loaded zein-tea saponin nanoparticles prepared by antisolvent co-precipitation and precipitation. *Food Chemistry*, Article 133224.
Liu, N., & Park, H. J. (2009). Chitosan-coated nanoliposome as vitamin E carrier. *Journal of Microencapsulation, 26*(3), 235–242.
Liu, Q., Jing, Y., Han, C., Zhang, H., & Tian, Y. (2019). Encapsulation of curcumin in zein/caseinate/sodium alginate nanoparticles with improved physicochemical and controlled release properties. *Food Hydrocolloids, 93*, 432–442.
Lohcharoenkal, W., Wang, L., Chen, Y. C., & Rojanasakul, Y. (2014). Protein nanoparticles as drug delivery carriers for cancer therapy. *BioMed Research International, 2014*.
Luo, Y., Zhang, B., Whent, M., Yu, L. L., & Wang, Q. (2011). Preparation and characterization of zein/chitosan complex for encapsulation of α-tocopherol, and its in vitro controlled release study. *Colloids and Surfaces B: Biointerfaces, 85*(2), 145–152.
McClements, D. J. (2015). Emulsion stability. *Food emulsions* (pp. 314–407). CRC Press.
Medina, E., Caro, N., Abugoch, L., Gamboa, A., Díaz-Dosque, M., & Tapia, C. (2019). Chitosan thymol nanoparticles improve the antimicrobial effect and the water vapour barrier of chitosan-quinoa protein films. *Journal of Food Engineering, 240*, 191–198.
Nasrollahzadeh, M., Sajadi, S. M., Sajjadi, M., & Issaabadi, Z. (2019). Applications of nanotechnology in daily life. *Interface Science and Technology, 28*, 113–143.
Nowack, B., & Bucheli, T. D. (2007). Occurrence, behavior and effects of nanoparticles in the environment. *Environmental Pollution, 150*(1), 5–22.
Oymaci, P., & Altinkaya, S. A. (2016). Improvement of barrier and mechanical properties of whey protein isolate based food packaging films by incorporation of zein nanoparticles as a novel bionanocomposite. *Food Hydrocolloids, 54*, 1–9.
Park, C.-E., Park, D.-J., & Kim, B.-K. (2015). Effects of a chitosan coating on properties of retinol-encapsulated zein nanoparticles. *Food Science and Biotechnology, 24*(5), 1725–1733.
Pauluk, D., Padilha, A. K., Khalil, N. M., & Mainardes, R. M. (2019). Chitosan-coated zein nanoparticles for oral delivery of resveratrol: Formation, characterization, stability, mucoadhesive properties and antioxidant activity. *Food Hydrocolloids, 94*, 411–417.
Putri, D. C. A., Dwiastuti, R., & Marchaban, A. K. N. (2017). Optimization of mixing temperature and sonication duration in liposome preparation optimasi suhu pencampuran dan durasi sonikasi dalam pembuatan liposom. *Jurnal Farmasi Sains dan Komunitas, 14*(2), 79–85.
Sapsford, K. E., Tyner, K. M., Dair, B. J., Deschamps, J. R., & Medintz, I. L. (2011). Analyzing nanomaterial bioconjugates: A review of current and emerging purification and characterization techniques. *Analytical Chemistry, 83*(12), 4453–4488.
Silva, H. D., Cerqueira, M.Â., & Vicente, A. A. (2012). Nanoemulsions for food applications: Development and characterization. *Food and Bioprocess Technology, 5*(3), 854–867.
Squillaci, G., Apone, F., Sena, L. M., Carola, A., Tito, A., Bimonte, M., Lucia, A. D., Colucci, G., Cara, F. L., & Morana, A. (2018). Chestnut (Castanea sativa Mill.) industrial wastes as a valued bioresource for the production of active ingredients. *Process Biochemistry, 64*, 228–236.
Tapia-Hernández, J. A., Rodríguez-Felix, F., Juárez-Onofre, J. E., Ruiz-Cruz, S., Robles-García, M. A., Borboa-Flores, J., Wong-Corral, F. J., Cinco-Moroyoqui, F. J., Castro-Enríquez, D. D., & Del-Toro-Sánchez, C. L. (2018). Zein-polysaccharide nanoparticles as matrices for antioxidant compounds: A strategy for prevention of chronic degenerative diseases. *Food Research International, 111*, 451–471.
Tsai, Y.-H., Yang, Y.-N., Ho, Y.-C., Tsai, M.-L., & Mi, F.-L. (2018). Drug release and antioxidant/antibacterial activities of silymarin-zein nanoparticle/bacterial cellulose nanofiber composite films. *Carbohydrate Polymers, 180*, 286–296.
Yang, Z., McClements, D. J., Peng, X., Xu, Z., Meng, M., Chen, L., & Jin, Z. (2023). Fabrication of zein–carboxymethyl cellulose nanoparticles for co-delivery of quercetin and resveratrol. *Journal of Food Engineering, 341*, Article 111322.
Yapıcı, H. H., Baygar, T., Metin, C., & Alparslan, Y (2015). Günlük ağaci (liquidambar orientalis) yapraklarindan elde edilen ekstraktin kültür levreğinin (dicentrarchus labrax) raf ömrü ve et kalitesi üzerine etkisi. *Journal of Food and Health Science Hasanhocaoğlu Yapıcı, 1*(4), 166–177. et al.
Yüksel, F. (2013). Gıda teknolojisinde ultrases uygulamaları. *Gıda Teknolojileri Elektronik Dergisi, 8*(2), 29–38.
Zhang, F., Khan, M. A., Cheng, H., & Liang, L. (2019). Co-encapsulation of α-tocopherol and resveratrol within zein nanoparticles: Impact on antioxidant activity and stability. *Journal of Food Engineering, 247*, 9–18.
Zhang, S., & Han, Y. (2018). Preparation, characterisation and antioxidant activities of rutin-loaded zein-sodium caseinate nanoparticles. *PLoS One, 13*(3), Article e0194951.
Zhang, Y., Niu, Y., Luo, Y., Ge, M., Yang, T., Yu, L. L., & Wang, Q. (2014). Fabrication, characterization and antimicrobial activities of thymol-loaded zein nanoparticles stabilized by sodium caseinate–chitosan hydrochloride double layers. *Food Chemistry, 142*, 269–275.
Zhong, Q., Jin, M., Xiao, D., Tian, H., & Zhang, W. (2008). Application of supercritical anti-solvent technologies for the synthesis of delivery systems of bioactive food components. *Food Biophysics, 3*(2), 186–190.